IBRO Neuroscience Reports 21 (2026) 542–558

Contents lists available at ScienceDirect

IBRO Neuroscience Reports

journal homepage: www.sciencedirect.com/journal/IBRO-Neuroscience-Reports

Behavioural, neurochemical, and neurohistological effects of bisphenol A and vanadium following chronic co-administration in mice

Damilare A. Adekomi [a,*], Hammed A. Ajani [a], Ruqayyah Y. Ibiyeye [b], Adesina O. Adekeye [c], Linus A. Enye [c], Edem E. Edem [c], Adebiyi A. Adegoke [d], Omowumi O. Adewale [e], Ebenezer IO. Ajayi [e], Temidayo D. Adeniyi [f], Opeyemi S. Osuntokun [g], Olumayowa K. Idowu [a], Moses A. Hamed [h], Babatunde J. Dare [i], Adewale V. Aderemi [j], Dayo R. Omotoso [k], Tope G. Atere [j], Dare E. Babatunde [l], Joshua H. Ojo [l], Gideon B. Ojo [l], Anifat T. Adekilekun [m]

[a] Department of Anatomy, Neuroscience and Cell Biology Unit, Faculty of Basic Medical Sciences, College of Health Sciences, Osun State University, Osogbo, Nigeria
[b] Department of Anatomy, Kwara State University, Malete, Kwara State, Nigeria
[c] Department of Anatomy, College of Medicine and Health Sciences, Afe Babalola University, Ado-Ekiti, Ekiti State, Nigeria
[d] Department of Anatomy, Endocrinology Research Unit, Faculty of Basic Medical Sciences, College of Health Sciences, Osun State University, Osogbo, Nigeria
[e] Department of Biochemistry, Faculty of Basic and Applied Sciences, Osun State University, Osogbo, Nigeria
[f] Department of Medical Laboratory Science, Faculty of Basic Clinical Sciences, University of Ilorin, Ilorin, Nigeria
[g] Department of Health and Social Care, Mont Rose College of Management and Sciences, Buckinghamshire New University, East London, United Kingdom
[h] Brainwill Laboratory Limited, Osogbo, Osun State, Nigeria
[i] Department of Anatomy, Anthropometry and Forensic Science Unit, Faculty of Basic Medical Sciences, College of Health Sciences, Osun State University,, Osogbo, Nigeria
[j] Department of Medical Biochemistry, Faculty of Basic Medical Sciences, College of Health Sciences, Osun State University, Osogbo, Nigeria
[k] Department of Anatomy, Redeemer's University, Ede, Osun State, Nigeria
[l] Department of Anatomy, Bowen University, Iwo, Osun State, Nigeria
[m] Cincinnati Children's Hospital Medical Center, OH, United States

ARTICLE INFO

Keywords:
Xenobiotic
Transition metals
Plasticizers
Prefrontal cortex
Neurocognition

ABSTRACT

Bisphenol A (BPA) and vanadium are industrial chemicals known to disrupt hormones and cause neurotoxicity. BPA is commonly found in food packaging and poses risks to human health through various exposure routes, while vanadium exposure can occur near power plants. Both chemicals induce oxidative stress, disrupt neurotransmission, and cause neuronal damage, yet research on their combined effects is limited. To examine the behavioral, neurochemical, and neurohistological changes associated with co-exposure to BPA and vanadium, we utilized 40 male BALB/c mice, divided into four groups: the control group, the BPA-exposed group, the vanadium-exposed group, and the BPA + vanadium co-exposed group. Mice in the control group received dimethyl sulfoxide (DMSO) only. The BPA-exposed group was administered 10 μg/kg bw/day of BPA, while the vanadium-exposed group received 1.2 mg/kg bw/day of vanadyl sulphate. Mice in the BPA + vanadium co-exposed group received both 10 μg/kg bw/day of BPA and 1.2 mg/kg bw/day of vanadyl sulphate. Each group underwent this oral administration daily for 56 consecutive days. Moreover, we conducted behavioral, histological and neurochemical analyses on the prefrontal cortex of the mice. Our findings revealed that co-exposure to BPA and vanadium significantly exacerbated impairments in behavioral and neurochemical indicators. Notably, the histoarchitectural profile of the prefrontal cortex indicated evidence of neuronal cell death. In conclusion, our study suggests that co-exposure to BPA and vanadium correlates with detrimental effects on behaviors associated with the prefrontal cortex, alongside substantial neurochemical disruptions and compromised structural integrity.

* Corresponding author.
E-mail address: adedayo.adekomi@uniosun.edu.ng (D.A. Adekomi).

https://doi.org/10.1016/j.ibneur.2026.01.015
Received 26 June 2025; Received in revised form 31 December 2025; Accepted 28 January 2026
Available online 4 February 2026

Introduction

The public health concerns surrounding transition metals and/or endocrine disruptors arise primarily from their reported disruption of cellular components, organogenesis, and crucial chemico-biological and metabolic processes in both herbage and vertebrates through the alteration of normal organo-enzyme pathways and physiological processes (Duffus, 2002). Published reports have shown that unregulated mitotic division and tissue damage, precipitated by environmental toxins, can contribute to neurological deficits by impeding normal tissue formation and by disrupting the normal functional integrities of the developing tissues of the central nervous system (Wang and Shi, 2001; Manto, 2012; Lawal et al., 2023).

Bisphenol A (BPA) is the main component in producing polycarbonate plastics and epoxy resins as an industrial chemical. BPA-laden materials are common in everyday use items, including food-related ones such as thermo-plastic containers (Geens et al., 2012; Caballero-Casero et al., 2016). Research by John and colleagues (2019) indicates that BPA is a recognized endocrine disruptor. Depending on the duration of exposure, environmental contaminants, causing various degrees of exposure in humans and living organisms, can reach toxic levels and produce oxidative dysfunctions through the development of redox imbalance, autoxidation of lipid, and structural alterations of DNA via nucleotide base modifications, thereby inhibiting the mechanisms involved in the synthesis and repair of DNA (Clancy et al., 2012; Zhang et al., 2016; Zhenkun et al., 2017; Durovcova et al., 2018). BPA, found in numerous consumer items, is known to enter the body via the nasal, oral, and dermal routes, resulting in unsafe amounts being observed in the urine of numerous population groups (John et al., 2019; Ma et al., 2019). The rising use of BPA has led to its presence in various environmental media such as processed foods, municipal water, effluent, and excretory products (Huang et al., 2012; Yang et al., 2020; Chen et al., 2021; Banaderakhshan et al., 2022; Manzoor et al., 2022). The severity of BPA pollution is becoming alarming in the human environment. BPA, in combination with transition metals, is commonly found together in both the ecosystem and food sources. It is necessary to investigate the toxicities of their mixtures.

Geens et al. (2012) identified oral, transdermal, and inhalation as some of the recognizable ways through which BPA enters the human body. BPA, as reported by Kawato (2004), is known to aggravate reproductive dysfunctions, cancer, thyroid deformities, and cognitive impairments due to its deleterious effects. Aging and various factors, including toxins, exposure to herbicides and/or pesticides, injuries to the head, and genetic predisposition, contribute to cognitive impairment (Chin-Chan et al., 2015). In a study by Inadera (2015), it was observed that exposure to different doses of BPA crosses the blood-brain barrier, resulting in impaired cognitive behaviors, including aggression, drug dependency, and hyper-reactivity, among other learning and memory deviations.

The metallic element Vanadium occurs naturally in the environment and is utilized for various commercial purposes, including manufacturing pesticides, sulphuric acid, hardening steel, and catalysis in materials production (Pessoa et al., 2015; Juan et al., 2021). Both the mining of transition metals and the combustion of vanadium-containing fuel oils contribute to an increase in vanadium exposure (Fatola et al., 2019). Studies show vanadium's potential to treat hypoglycemia, cancer, and parasitic infections (Moskalyk and Alfantazi, 2003; Gambino, 2011; Huang et al., 2014; León et al., 2014; Mucci et al., 2020).

Humans and animals can be exposed to vanadium compounds found in food, water, soil, and air (Habib and Ibrahim, 2011; Rozzo et al., 2017; Igado et al., 2020). Vanadium compounds can build up in various organs in the human body (Imtiaz et al., 2015; Brown et al., 2019).

Rodents exposed to a low dose of vanadium have been reported to show dysfunctional locomotion and impaired learning and memory. Studies by Sanchez et al. (1998) and Sun et al. (2017) highlight locomotor deficits, while research by Avila-Costa et al. (2006), Azami et al. (2012), and Folarin et al. (2016). Although vanadium is considered a neurotoxic metal, its compounds hold therapeutic potential. For example, vanadium compounds may help alleviate conditions like diabetes due to their insulin-like properties, as well as certain aspects of Alzheimer's disease (Amaral et al., 2023; Dayanand et al., 2024). According to Fatola et al. (2019), most published research reports that examined vanadium have used low to higher doses. Factory workers are at a higher risk of inhaling a significant proportion of vanadium, while the population at large typically consumes minimal amounts through diet or drinking groundwater (He et al., 2020).

Extensive research has thoroughly examined the individual toxic effects of bisphenol A (BPA) and various transition metals. BPA, widely recognized as an endocrine disruptor, poses significant health risks beyond hormonal interference; it has been shown to exhibit genotoxic properties (Balabanic et al., 2021) and adversely affect reproductive health (Baralic et al., 2021; Dagher et al., 2021), nervous system function (Fu et al., 2020; Guo et al., 2020), developmental processes (Chen et al., 2019; Zhou et al., 2020), and immune responses (Oehlmann et al., 2009; Gowder, 2013). In contrast, transition metals, known for their persistent nature, can accumulate in human tissues due to their long biological half-lives. This accumulation can lead to serious health issues in vital organs such as the brain, kidneys, and liver (Mansour, 2014). Given the challenges associated with lengthy experimental timelines and the inconsistent results often linked to animal testing, it is crucial to consider that BPA and transition metals frequently coexist in our environment and food sources. Consequently, further investigation is needed to understand the toxic effects of their mixtures, which may pose even greater risks to human health than their entities. From our study, BPA and vanadium were detected in the prefrontal cortex, which implies that BPA and vanadium may enter the blood-brain barrier and manipulate neurons in the prefrontal cortex.

In several animal models, exposure to environmental toxicants alters the metabolism of neurotransmitters within brain topographies (Ścibior et al., 2020). These neurotransmitters include acetylcholine, dopamine, glutamate, GABA, and serotonin, each capable of aggravating behavioral and cognitive abnormalities (Barceloux, 1999). To investigate the neurotoxicity mechanisms of BPA and vanadium, it is important to identify associated behavioral changes and mitochondrial dysfunction.

The prefrontal cortex plays a crucial role in regulating and controlling various higher executive functions, such as logical reasoning and decision-making (Nabi and Tabassum, 2022). However, the effects of exposure to the combination of BPA and vanadium on the prefrontal cortex have not yet been studied.

The progressive loss of morpho-physiological features of the neurons, often accompanied by neural suicide, leads to various disease conditions that influence cognitive operations and locomotion. Environmental toxicants contribute significantly to neuroinflammation and neuronal loss. Among these factors, toxicants, BPA, and vanadium are a well-known ecological toxin that causes neurodegeneration and negatively impact neurodevelopment and mental health (Liu et al., 2020). Despite extensive documentation of their neurotoxic effects, these substances are still widely used in various applications (Funahashi, 2017). BPA and vanadium are neurotoxicants that can cross the blood-brain barrier, causing oxidative stress (Tchounwou et al., 2012; Tran and Miyake, 2017), morphological damage, neurodegeneration, and cognitive impairment, especially in both developing and mature brains (Ma et al., 2019).

Higher executive and neurologic skills are dependent upon the prefrontal cortex (PFC), which comprises up to a third of the anterior component of the brain (Tchounwou et al., 2012). Research indicates that the intrinsic connections of the PFC form numerous links with other regions of the brain that are essential for cognitive processing (Rao Barkur and Bairy, 2015).

Long-term exposure to bisphenol A (BPA) and vanadium has been shown to potentially cause various morphological changes in neuronal structures and lead to neuronal cell death, as reported by Abd Elkader

and Al-Shami (2023) and Ladagu et al. (2023). Several studies have highlighted a concerning link between exposure to these substances and increased production of reactive oxygen species (ROS). For example, Meli et al. (2020) and Aureliano et al. (2023) have emphasized the role of ROS in mediating oxidative stress, which occurs when there is an imbalance between the production of these harmful species and the body's antioxidant defenses to neutralize them. An accumulation of reactive intermediates can damage different cellular components, resulting in the formation of secondary toxic compounds that worsen cellular stress. Importantly, ROS can activate various redox-sensitive transcription factors that are crucial for triggering the transcription of inflammatory genes, and this process leads to the release of a wide range of inflammatory mediators (Rauf et al., 2024). Besides promoting ROS production, increasing evidence links exposure to BPA and vanadium with the activation of apoptotic mechanisms (Aureliano et al., 2023; Wang et al., 2024). This is especially important because recent research shows a strong connection between mental and emotional health and changes in neurotransmitter levels and circulating inflammatory cytokines. Studies by Cui et al. (2024) and Sălcudean et al. (2025) suggest that higher levels of inflammatory cytokines are positively associated with cognitive deficits, fatigue, disrupted sleep patterns, and depression symptoms, as reported by Bansal et al. (2025). Despite these findings, the exact mechanisms through which co-exposure to BPA and vanadium impacts brain function are still not fully understood. Therefore, this study aims to explore the effects of chronic co-administration of BPA and vanadium on the prefrontal cortex of mice. The research examines anxiety-like behaviors, oxidative stress markers, apoptotic activity, neurotransmitter alterations, and the histological condition of the prefrontal cortex to better understand the potential neurotoxic effects of these substances.

Materials and methods

Ethical considerations and animal handling protocol

The scientific method employed in this study was certified (UNIOSUNAC/2024/0206) and permitted by the Ethical Committee on the Use and Care of Experimental Animals of Osun State University (Osogbo, Nigeria). The National Institutes of Health's Guide for the Care and Use of Laboratory Animals (NIH Publications No. 80–23) was followed in granting this approval. The study employed male BALB/c mice (N = 60) aged 10–13 weeks. Throughout the experiment, the mice were kept in temperature-controlled (23 ± 3°C) and humidity-controlled (52 ± 7 %) rooms with natural light-dark cycles. The mice were obtained from the rodent colony at Osun State University (Osogbo, Nigeria). They had unrestricted access to double-distilled water and rodent chows. Under veterinary supervision, we ensured a minimal number of animals were used.

Drugs and chemicals

Bisphenol A and vanadyl sulphate were purchased from Sigma-Aldrich. Stock solutions were freshly prepared every week. In our study, Bisphenol A (BPA) and vanadyl sulphate were first dissolved in dimethyl sulfoxide (DMSO), ensuring complete solubility before further dilution in a physiological saline solution consisting of 0.9 % sodium chloride. To maintain consistency across experimental groups, the mice used in the study were uniformly exposed to a DMSO concentration of 0.7 %. The stock solution was stored in amber bottles under refrigeration, and the dosing solution was prepared and administered daily.

Animal care, experimental groupings, and chemical exposures

The BALB/c mice used in this study (N = 40, 21–22 g) were assigned to 4 groups (n = 10): control, BPA, Vanadium, and BPA + Vanadium: the control group received only DMSO, the BPA group was administered a daily dose of 10 μg/kg bw/day of BPA, based on the findings from Zhu et al. (2024), the vanadium group was treated with vanadyl sulphate at a dosage of 1.2 mg/kg bw/day, as referenced in the work of Hussain Shah et al., 2016). Lastly, the combination group received both 10 μg/kg bw/day of BPA and 1.2 mg/kg bw/day of vanadyl sulphate. All administrations were orally done once daily for 56 days. Bisphenol A and vanadium are chemical substances that can infiltrate the human body through numerous routes, ranging from ingestion, inhalation, to dermal absorption. This exposure arises owing to the widespread use of these compounds in various daily products, which include plastics and coatings (Shelby, 2008). While studies have shown that subcutaneous injection might provoke more pronounced 'biochemico-physiological' responses in laboratory animal models compared to equivalent doses administered orally (Yang et al., 2015), this study selected the oral gavage, and the rationale behind this choice was that the primary mode of exposure for humans is through the consumption of contaminated foods, water, and beverages.

Behavioral protocols

The mice in the respective groups underwent a series of behavioral tests, including an open-field test (day 55) and an elevated plus maze test (day 56). Behavioral procedures were performed one hour after administration of the test substances.

Open-field behavioral test

The open-field test was used to evaluate anxiety, exploration, and motor activity levels in mice (Kraeuter et al., 2019; Petanjek et al., 2019). The chamber was a 40 × 40 × 40 cm square-shaped Plexiglas structure with a brightly lit interior, with the floor partitioned into central and peripheral zones on the floor (demarcated into 16 small grids). 300-second-long sessions were conducted for individual mice in the open-field arena. An overhead video camera was set up to record mouse movements in the arena. ANY-maze video tracking software (Version 7.00) was used to document the number of center entries (n), the percentage of time spent in the central zone, the mean distance traveled (m), the number of line crossings (n), total ambulatory time (sec.), and the number of rearing episodes. Rearing was defined as the behavior of mice when they maintain an upright posture without leaning against the wall.

Elevated plus maze

The elevated plus maze behavioral test is an invaluable and dependable technique for evaluating the anxiogenic and anxiolytic effects of various chemicals, metals, and pharmacological agents (Petanjek et al., 2019; Ge et al., 2023). This apparatus features two open arms, each measuring 50 × 10 cm, coupled with two closed arms of identical size, forming a 90° angle with a central platform measuring 5 × 5 cm, elevated 25 cm off the ground. In this precise methodology, individual mice from designated groups are carefully placed on the central platform, facing one of the open arms. They are permitted to navigate the maze for 300 s. An overhead camera, powered by ANY-maze tracking software (version 7.00), meticulously captures the mice's movements, enabling measurement of the time spent in both the open and closed arms of the maze.

Neurochemical analysis

The mice were euthanized using diethyl ether, and the isolated brains were thoroughly rinsed with 10 % w/v sodium phosphate buffer (pH 7.4). The prefrontal cortices were homogenized and centrifuged, and the supernatant collection was performed as described in the study of Ben-Azu et al. (2018) and Umukoro et al. (2023). The supernatant was used for the determination of the levels of SOD, catalase, GPx, GSH,

MDA, NK-κB, MAPK-14, nNOS, iNOS, COX-2, MPO, Bax, Bcl-2, caspase-3, AChE, serotonin, and dopamine. The respective concentrations of SOD, catalase, GPx, GSH, MDA, NK-κB, MAPK-14, nNOS, iNOS, COX-2, MPO, Bax, Bcl-2, caspase-3, AChE, serotonin, and dopamine from the prefrontal cortex were extrapolated from their standard curves.

Assessing the amount of superoxide dismutase (SOD)

Using a SOD test kit (E-BC-K020, Elabscience Biotechnology Co., Ltd.), the amount of the superoxide dismutase (SOD) enzyme was assessed in the supernatants from each mouse in the corresponding experimental groups. The reaction mixture contained 200 μL of substrate application solution, 20 μL of enzyme working solution, and 20 μL of the supernatant. After fully mixing the mixture, it was incubated for 20 min at 37°C. A microplate reader (Model 680; Bio-Rad Laboratories, CA, USA) was used to measure the absorbance at 450 nm. The data were represented as U/g tissue.

Measuring the level of catalase

The Bradford (1976) technique, cited in the work by Correa et al. (2001), was used to assess the catalase level in the supernatants from each mouse in the corresponding experimental groups. In short, an Eppendorf microcentrifuge was used to centrifuge the supernatants (20 μL) for 5 min at 15,000 rpm. The catalase level was measured using 15 μL aliquots of the supernatant. By tracking the drop in hydrogen peroxide absorbance at 240 nm, the catalase level was determined spectrophotometrically. The Lowry et al. (1951) technique was used to measure the protein levels in the supernatants, and the results were expressed as U/g protein.

Determination of the level of glutathione peroxidase (GPx)

With minor adjustments, the amount of glutathione peroxidase (GPx) in the supernatants from each mouse in the corresponding experimental groups was determined using the Rotruck et al. (1973) technique, which Adelakun et al. (2024) quoted. To put it briefly, the sample-containing reaction mixture was incubated for three minutes at 37°C. Following incubation, the mixture was centrifuged for five minutes at 3,000 rpm with 0.5 ml of 10 % trichloroacetic acid added. After adding 1 ml of 5,5′-dithiobis-(2-nitrobenzoic acid) solution and 2 ml of phosphate buffer to each of the resultant supernatants (15 μL), the absorbance at 412 nm was measured in comparison to a blank. U/g tissue was used to express the GPx findings.

Measuring reduced glutathione (GSH) levels

The level of reduced glutathione (GSH) was measured using the method described by Beutler et al. (1963). In brief, 4.5 ml of Ellman's reagent was combined with 0.5 ml of supernatant from each mouse in the corresponding experimental groups. A blank sample was created using 4.5 ml of Ellman's reagent and 0.5 ml of a diluted precipitating agent. GSH absorbs light at a wavelength of 412 nm. The results for GSH levels were expressed as units per gram of tissue (U/g tissue).

Determination of the level of malondialdehyde (MDA)

The malondialdehyde (MDA) level was measured in the supernatants from each mouse in the respective experimental groups using a lipid peroxidation assay kit (MAK568, Sigma-Aldrich). The procedure was conducted according to the manufacturer's instructions (Sigma-Aldrich). The supernatants were analyzed for MDA using a microplate reader (Model 680; Bio-Rad Laboratories, CA, USA) set to a wavelength of 553 nm. The results for MDA were expressed as nmol/100 mg tissue.

Determination of the level of activated p65 nuclear factor-kappa B subunit

Following the detailed protocols provided by the manufacturer, the Cell Signaling Technology PathScan (Cell Signaling Technology, Boston, MA) Phospho-NF-κB p65 (Ser536) Sandwich ELISA kit was employed to prepare and analyze the supernatants obtained from each mouse belonging to the various experimental groups. To initiate the process, microwells specifically coated with a high affinity phospho p65 (Ser536) mouse monoclonal antibody were filled with 40 μL of the extracted protein, followed by the addition of 60 μL of a sample diluent. This carefully prepared mixture was incubated overnight at a controlled temperature of 4°C to ensure optimal binding and stability. After the incubation period, the wells underwent a thorough washing step to remove any unbound substances. Subsequently, a rabbit monoclonal antibody conjugated with horseradish peroxidase was introduced to identify and bind to the phosphorylated NF-κB p65 protein that had been captured on the microwell surface. To facilitate the detection process, the 3,3′,5,5′-tetramethylbenzidine substrate was applied, leading to a distinct color change that indicated a successful reaction. Finally, a microplate reader (Model 680; Bio-Rad Laboratories, CA, USA) was utilized to accurately measure the absorbance at a wavelength of 450 nm. The findings of this analysis were then quantified and reported as ng/g of tissue.

Evaluation of cyclooxygenase-2 (COX-2) levels

To assess the levels of cyclooxygenase-2 (COX-2) in the experimental samples, we utilized the COX-2 assay ELISA kit (CSB-E12910m, Cusabio Life Sciences, Wuhan, China). This kit enabled us to quantify the COX-2 concentrations present in the supernatants collected from each mouse within their respective experimental groups. The measurement process was carried out at room temperature, following the detailed protocols provided by the manufacturer to ensure accuracy and reliability. After the assay was conducted, a microplate reader (Model 680; Bio-Rad Laboratories, CA, USA) was employed to measure the absorbance of the samples at a wavelength of 450 nm. The results were subsequently reported in terms of picograms per milliliter (pg/ml).

Assessment of Bax, Bcl-2, and caspase-3 activity

To evaluate the apoptotic processes within the experimental groups, we utilized a highly sensitive Enzyme-Linked Immunosorbent Assay (ELISA) kit, following the manufacturer's specific guidelines. This allowed us to determine the concentrations of the pro-apoptotic protein Bax (MM-1143H2, MeiMian, Yancheng, Jiangsu, China) as well as the anti-apoptotic protein Bcl-2 (MM-0306M2, MeiMian, Yancheng, Jiangsu, China) present in the supernatants obtained from each mouse. In addition, we employed a Caspase-3 assay kit (C1115, Beyotime Biotechnology, Shanghai, China) to ascertain the levels of this key apoptotic executor protein. For measuring the absorbance and quantifying the protein levels of Bax, Bcl-2, and Caspase-3, we used a microplate reader (Model 680; Bio-Rad Laboratories, CA, USA), optimized to read at a wavelength of 450 nm. The results obtained from these assays were reported as nanograms of protein per gram of tissue.

Determination of the level of acetylcholinesterase

The level of acetylcholinesterase enzyme in the supernatants from each mouse in the respective experimental groups was determined using a quantification ELISA kit (CSB-E17521m, Cusabio Life Sciences, Wuhan, China). The analysis was conducted at room temperature following the method established by Ellman et al. (1961). The absorbance of each well was measured at a wavelength of 450 nm using a microplate reader (Model 680; Bio-Rad Laboratories, CA, USA), and the results were expressed in ng/mg protein.

Determination of the levels of serotonin

Serotonin levels were measured in the supernatants from each mouse in the respective experimental groups. The level of serotonin was determined at room temperature using an ELISA kit (KA2518, Abnova, Taipei, Taiwan), following the manufacturer's protocols. The absorbance of each well was measured at a wavelength of 450 nm using a microplate reader (Model 680; Bio-Rad Laboratories, CA, USA), and the results were expressed in μg/ml.

Determination of the levels of dopamine

The dopamine levels in the supernatants from each mouse in the respective experimental groups were determined by rapidly dissecting the prefrontal cortex on ice. Following the manufacturer's instructions, we used a mouse dopamine ELISA kit (CSB-E08661m, Cusabio Life Sciences, Wuhan, China) for this analysis. The absorbance of each well was measured at a wavelength of 450 nm using a microplate reader (Model 680; Bio-Rad Laboratories, CA, USA), and the results were expressed in μg/ml.

Analysis of BPA concentration in the prefrontal cortices of the mice

To measure the concentration of BPA in the prefrontal cortex, a UPLC-MS/MS system equipped with an ESI mass spectrometer was employed. The process began with the careful homogenization of the prefrontal brain tissue with 400 μl of methanol. This mixture was then centrifuged for five minutes at a temperature of 4°C and a high rotational speed of 13,000 rpm to separate the soluble components from the solid matrix. Following centrifugation, 200 μl of the resulting supernatant was evaporated at ambient temperature to concentrate the BPA. The dried residue was reconstituted in 40 μl of methanol, thoroughly vortexed to ensure homogeneity, and subjected to another round of centrifugation for five minutes at 4°C and 13,000 rpm. For the measurement of BPA, a normal-phase liquid chromatography (LC) technique was utilized, featuring two mobile phase solutions: Solution A, which consisted of water with 0.05 % ammonium hydroxide, and Solution B, a methanol solution with 0.1 % formic acid. The mobile phases were calibrated to flow at a rate of 0.3 ml/min, following a precise gradient setup. The gradient was configured as follows: from 0 to 0.2 min, the mobile phase composition was 90 % A and 10 % B; from 1 to 1.5 min, it shifted to 2 % A and 98 % B; and finally, from 1.5 to 2 min, it returned to the initial ratio of 90 % A and 10 % B.

Analysis of vanadium content in the prefrontal cortices of the mice

The analysis of vanadium content in the prefrontal cortices of the experimental mice was determined using the method of Sun et al. (2017). Briefly, the Varian SpectroAA-240Z flameless graphite furnace atomic absorption spectrophotometer was used to measure the levels of vanadium in the prefrontal cortices of the experimental mice. In the MARSXpress microwave-accelerated reaction system, the prefrontal cortices were treated with 10.0 ml of ultrapure concentrated HNO_3 (Sinopharm Chemical Reagent Co., Ltd, AR Select grade) for 4 h. The tubes were placed on an electric heating plate to evaporate off most of the nitric acid at the end of digestion. The samples were diluted to 2.0 ml with 0.5 % nitric acid. The standard curves were daily prepared afresh in a 0.5 % nitric acid solution within a 0–10 μg/L concentration range.

Histological procedure

Mice in the respective experimental groups were anesthetized using ether. Following this, the mice were perfused with phosphate-buffered saline (pH 7.4), and the whole brains were harvested and fixed in freshly prepared 10 % neutral buffered formalin. The brains were then processed using the routine method for paraffin wax embedding for paraffin-embedded tissue blocks. A 5 μm-thick section of the prefrontal cortex was obtained using a microtome (Leica, Germany). These sections were subjected to further processing for H&E staining and Golgi staining. Digital images of the stained sections were captured using an AxioCam MRc camera attached to a Zeiss Axioscope A1 microscope at 400x magnification.

H&E staining procedure

To prepare the prefrontal cortices for staining, we divided them into sections and placed them on glass slides in a staining slide rack. First, we removed the wax by soaking the slides in xylene for five minutes, changing the xylene twice. Next, we hydrated the sections by rinsing them for two minutes each in 100 %, 90 %, and 70 % alcohol. Then, we washed them for three minutes under running tap water to remove any remaining alcohol. After this, we stained the slides with hematoxylin for five minutes. We rinsed them again for three minutes in running water to allow the color to develop, then counterstained them with eosin for three minutes. Following another rinse in water, we dehydrated the sections using increasing alcohol concentrations (50 %, 70 %, 90 %, and 100 %) for one minute each. Finally, after cleaning the slides quickly in xylene and drying them in an oven at 80°C for 60 s, we covered the sections with a microscopic cover glass using Distrene Plasticizer Xylene (DPX) mountant (Bancroft and Gamble, 2008). Photomicrographs obtained from H&E-stained sections of the prefrontal cortices of representative mice from the different experimental groups were analyzed using ImageJ (v. 1.49), a software package developed by the National Institutes of Health. Analysis of observable histopathological deviations in the prefrontal cortices was performed on five distinct sections from layers II and III in each mouse, in accordance with established diagnostic guidelines outlined in the International Harmonization of Nomenclature and Diagnostic Criteria for Lesions in Rats and Mice (Bradley et al., 2020). This helped to maintain consistency and reliability in our findings. The histopathological assessment was targeted at identifying neurons with features of neuronal degeneration, with the percentage of affected neurons calculated using the following formula:

$$\frac{Numberofneuronswithfeaturesofneurodegeneration}{Totalnumberofneuronsassessed} \times 100$$

Golgi staining procedure

The prefrontal cortices were placed in a 3 % potassium bichromate solution for 5 days. To block light, we covered the specimen bottles with aluminum foil and stored them in a dark chamber. We changed the solutions daily. After this initial treatment, we transferred the tissue blocks to a 2 % silver nitrate solution for 3 days at room temperature. We also kept this solution away from light and used fresh solutions every day. Before placing the blocks in the silver nitrate solution, we used filter paper to soak up any extra liquid. We changed the silver nitrate solution several times until we no longer saw any brown precipitate. To dehydrate the tissues, we passed them through 70 %, 90 %, and 100 % alcohol, followed by xylene, spending 5 min in each. Then, we infiltrated the tissues with molten wax at 56°C for 30 min. We embedded the tissues in paraffin wax using a Leica wax dispenser (EG 1150 H, USA) and cooled them with a Leica cooling unit (EG 1150 C, USA). We cut the sections to a thickness of 60 μm with a Leica microtome (RM 2135) and mounted them on precleaned micro-slides (26 × 76 × 1.0 mm) using Leica X-tra adhesive. After air-drying the slides for 10 min, we coverslipped them with DPX (Femi-Akinlosotu et al., 2019).

Morphometry of Golgi-stained neurons

The detailed image stacks of Golgi-fixed sections from the prefrontal cortex of experimental animals were obtained using the Leica Application Suite version 3.3.0 (Switzerland). Each two-dimensional image

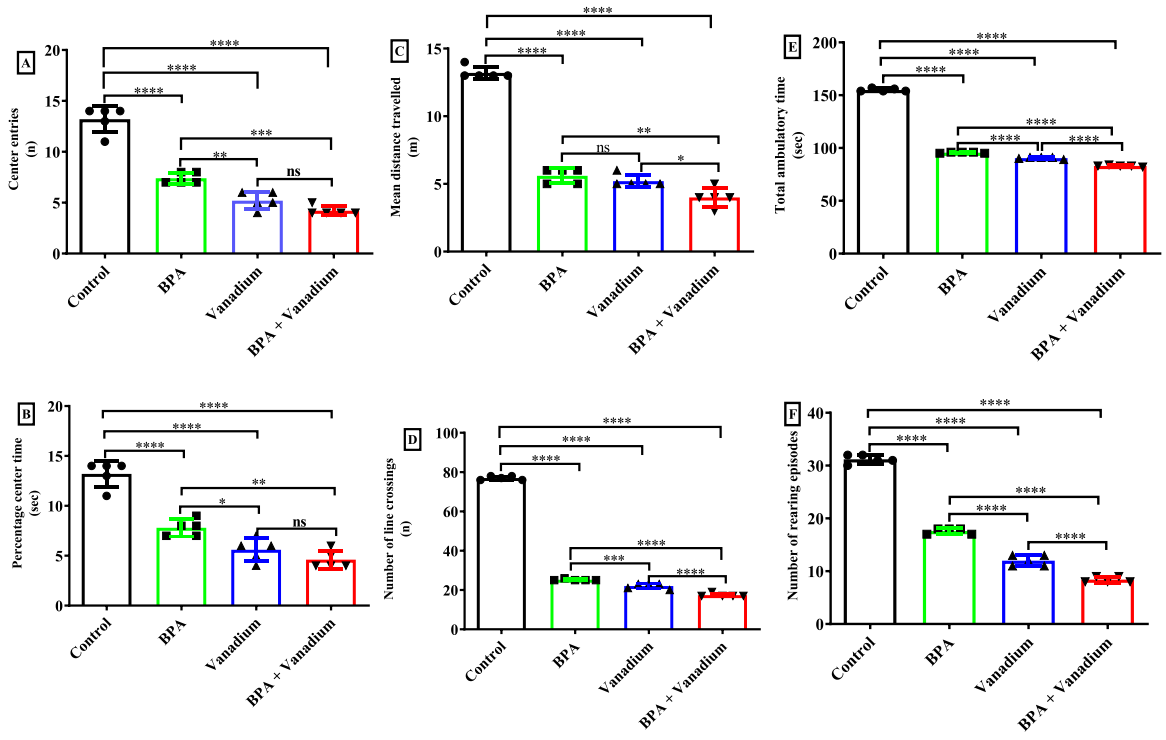

Fig. 1. The effect of BPA and/or vanadium on exploratory activities in mice assessed in the open-field test. (A) center entries, (B) percentage center time, (C) mean distance travelled, (D) number of crossings, (E) total ambulatory time, and (F) number of rearing episodes. Data obtained was evaluated using one-way ANOVA (*P < 0.05, **P < 0.01, ***P < 0.001, ***P < 0.0001). The values are presented as means ± SD (n = 5/group).

stack captured a resolution of 640 pixels × 480 pixels at a magnification of 40 × , specifically focusing on the intricate structures of the basal dendrites, and to ensure the selection of a homogenous neuronal population for our analysis, we adhered to specific criteria for the neurons established by Xiong et al. (2013) and Femi-Akinlosotu et al. (2019). In the first instance, we ensured that the cell body and all associated dendrites were fully impregnated, allowing for clear visualization of their morphology. Secondly, we ensured that the neurons were sufficiently isolated from surrounding neurons to avoid interference in our assessment, and lastly, we made sure that all dendrites were visible within the same plane of focus, enhancing the accuracy of our measurements. For the quantification of basal dendrite length, we calculated the mean length based on 10 basal dendrites from each animal, specifically from layer II-III of the prefrontal cortex. This analysis was conducted using ImageJ software (v. 1.49), ensuring precise measurements of these critical neuronal structures.

Statistical processing of data obtained

The data collected were analyzed using GraphPad Prism 8 software (v. 8.2, San Diego, USA). To assess the distribution characteristics of the variables and the homogeneity of variance, a Shapiro–Wilk test was conducted. Differences between groups were evaluated using one-way analysis of variance (ANOVA) followed by Tukey's post hoc test. The results were summarized as the mean accompanied by the standard deviation. A significance level was established at p-value < 0.05.

Results

Effect of bisphenol A, vanadium, and their combination on exploratory activities in the open-field test (Fig. 1A-F)

We investigated the effects of exposure to BPA, vanadium, and their combination on exploratory behaviors in mice using the open-field test. We examined various measures, including the frequency of mouse entries into the center, the duration of their stay, the distance traveled, the number of lines crossed, total walking time, and the frequency of rearing up. Our analysis showed that exposure to BPA, vanadium, and their combination significantly reduced the number of center entries in the open field test ([F(3, 16) = 111.9, $p < 0.0001$, Fig. 1A). The follow-up tests indicated that the treatment groups had fewer center entries than the control group. We also found that these exposures significantly affected the percentage of time spent in the center of the open field chamber ([F(3, 16) = 65.54, $p < 0.0001$], Fig. 1B). The follow-up analysis showed a clear difference in center time between the control group and those treated with BPA, vanadium, or both. Exposure to BPA, vanadium, and their combination also lessened the average distance traveled compared to the control group ([F(3, 16) = 292.4, $p < 0.0001$], Fig. 1C). Additionally, treatment with BPA, vanadium, and the combination significantly reduced the number of line crossings compared to the control group ([F(3, 16) = 3897, $p < 0.0001$], Fig. 1D). Total walking time was also significantly lower in mice exposed to BPA, vanadium, and both compared to the control group ([F(3, 16) = 6077, $p < 0.0001$], Fig. 1E). Finally, our analysis showed that exposure to BPA, vanadium, and their combination greatly decreased the number of rearing episodes compared to the control group ([F(3, 16) = 871.3, $p < 0.0001$], Fig. 1F).

Effect of bisphenol A, vanadium, and their combination on anxiety-like behavior in the elevated plus maze test (Fig. 2A-B)

To study how BPA, vanadium, and their combination affect anxiety-like behaviors, we tested mice using the elevated plus maze. We examined how much time the mice spent in the open and closed arms of the maze. The results showed that exposure to BPA, vanadium, and their combination changed the time spent in the closed and open arms significantly. This was confirmed by a two-way ANOVA test, which gave a result of [F(3, 16) = 94.46, $p < 0.0001$], as seen in Fig. 2A. Further analysis showed that mice in the BPA, vanadium, and BPA + vanadium groups spent significantly more time in the closed arm compared to the

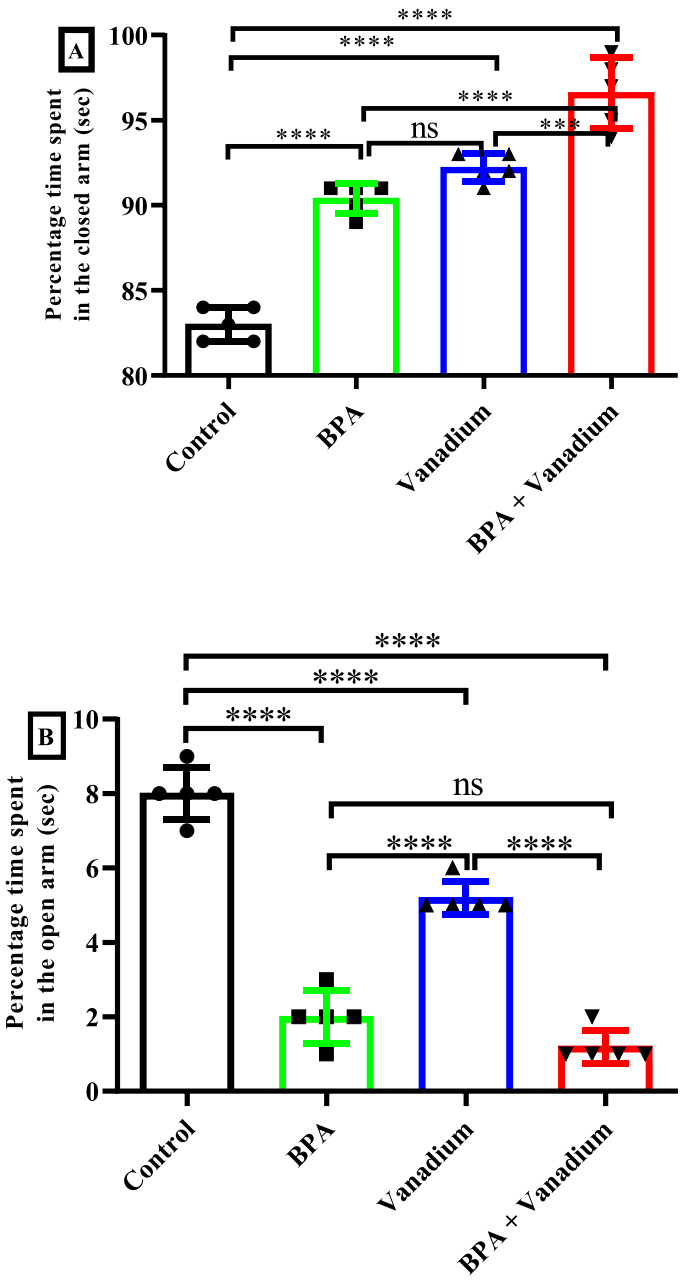

Fig. 2. The effect of BPA and/or vanadium on anxiety-related behavior in the mice assessed in the elevated plus maze test. (A) Percentage time spent in the closed arm, and (B) Percentage time spent in the open arm. The data obtained was analyzed using one-way ANOVA (***p < 0.001, ****p < 0.0001). Data is expressed as mean ± SD (n = 5 mice/group).

control group. We also found that the exposure to these substances affected the time spent in the open arm. The two-way ANOVA indicated this with a result of [F(3, 16) = 139.2, $p < 0.0001$], shown in Fig. 2B. The post hoc analysis revealed a significant difference in the time spent in the center of the maze between the control group and the groups that were exposed to BPA, vanadium, or both.

Effect of bisphenol A, vanadium, and their combination on the levels of antioxidant and oxidant markers in the prefrontal cortex (Fig. 3A-E)

Exposure to BPA and vanadium, alone or together, greatly reduced the levels of important antioxidants and increased the levels of deleterious substances in the prefrontal cortex of mice. Specifically, the levels of superoxide dismutase in the group of mice exposed to BPA, vanadium, and the combination of BPA + vanadium were significantly reduced compared with the control group F (3, 16) = 273.7, p < 0.0001, Fig. 3A). Additionally, the levels of catalase in the group of mice exposed to BPA, vanadium, and the combination of BPA + vanadium were significantly reduced compared with the control group (F (3, 16) = 559.7, p < 0.0001, Fig. 3B) Similarly, the levels of glutathione peroxidase in the group of mice exposed to BPA, vanadium, and the combination of BPA + vanadium were significantly reduced compared with the control group (F (3, 16) = 737.8, p < 0.0001, Fig. 3C). Also, the levels of glutathione were significantly reduced in the BPA-treated group, vanadium, and the combination of BPA + vanadium compared with the control group (F (3, 16) = 5617, p < 0.0001, Fig. 3D). Additionally, the level of malondialdehyde was significantly upregulated in the groups of mice exposed to BPA, vanadium, and the combination of BPA + vanadium relative to the control group (F (3, 16) = 2021, p < 0.0001, Fig. 3E).

Effect of bisphenol A, vanadium, and their combination on the levels of inflammatory and pro-inflammatory cytokines in the prefrontal cortex (Fig. 4A-F)

We found that the levels of inflammatory and pro-inflammatory cytokines studied were higher in the prefrontal cortex of mice exposed to BPA, vanadium, and a combination of both compared to the control group. Specifically, the levels of activated p65 NF-κB were significantly upregulated in the groups of mice exposed to BPA, vanadium, and the combination of BPA + vanadium compared to the control group (F (3, 16) = 239.2, p < 0.0001, Fig. 4A). In the same vein, the levels of MAPK-14 in the mice exposed to BPA, vanadium, and the combination of BPA + vanadium compared to the control group (F (3, 16) = 939.1. p < 0.0001, Fig. 4B). The levels of nNOS were significantly upregulated in the groups of mice exposed to BPA, vanadium, and the combination of BPA + vanadium compared to the control group (F (3, 16) = 3921, p < 0.0001, Fig. 4C). As presented in Fig. 4D (F (3, 16) = 6797, p < 0.0001), it was observed that the levels of iNOS were significantly upregulated in the groups of mice exposed to BPA (134.00 ± 0.71), vanadium, and the combination of BPA + vanadium compared to the control group. Our result showed that the levels of COX-2 were significantly upregulated in the groups of mice exposed to BPA, vanadium, and the combination of BPA + vanadium compared to the control group (F (3, 16) = 6797, p < 0.0001, Fig. 4E). Furthermore, the levels of MPO were significantly upregulated in the groups of mice exposed to BPA, vanadium, and the combination of BPA + vanadium (46.40 ± 0.89) compared to the control group (F (3, 16) = 1311, p < 0.0001, Fig. 4F) levels all increased significantly.

Effect of bisphenol A, vanadium, and their combination on the levels of apoptotic and anti-apoptotic markers in the prefrontal cortex (Fig. 5A-C)

The levels of Bax, Bcl-2, and caspase-3 are shown in Fig. 5A-C. Compared to the control group, the levels of Bax were significantly upregulated in the BPA-exposed group, vanadium-exposed, and the BPA + vanadium co-exposed (F(3, 16) = 981.9, $p < 0.0001$, Fig. 5A). Conversely, the levels of Bcl-2 were significantly upregulated in the control group compared with the BPA-exposed, vanadium-exposed, and the BPA + vanadium co-exposed (F(3, 16) = 20657, $p < 0.0001$, Fig. 5B). From the analyzed statistical data obtained from the study, we observed that the levels of caspase-3 were significantly downregulated in the prefrontal cortex of the mice in the control group compared with the BPA-exposed, vanadium-exposed, and the BPA + vanadium co-exposed (F(3, 16) = 1214, $p < 0.0001$, Fig. 5C).

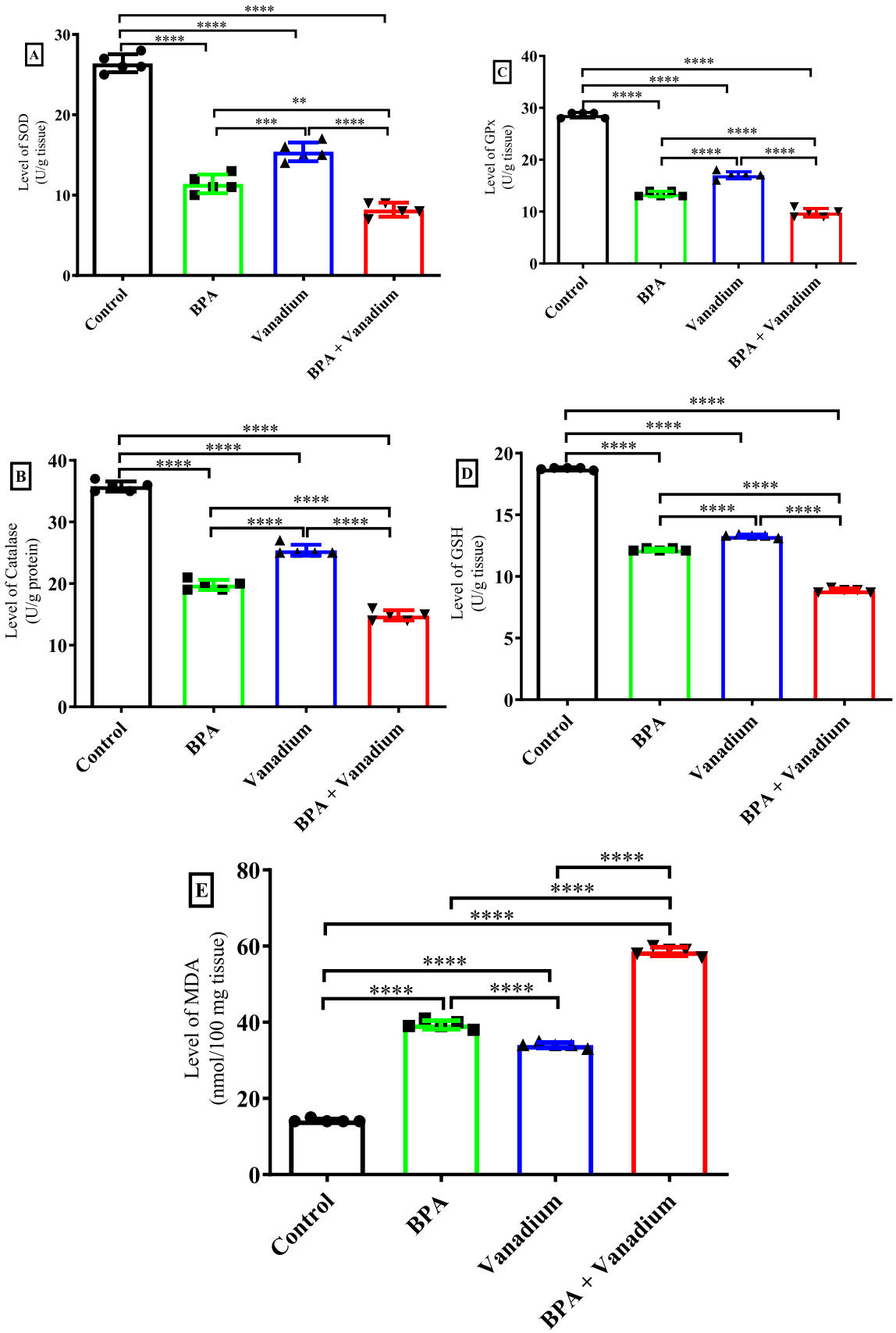

Fig. 3. The effect of BPA and/or vanadium on the levels of antioxidant and oxidant markers in the prefrontal cortex of the mice. Data is expressed as mean ± SD (n = 5). (A) level of SOD, (B) level of catalase, (C) level of GPx, (D) level of GSH, and (E) level of MDA. The data obtained was analyzed using one-way ANOVA (**P < 0.01, ***P < 0.001, ***P < 0.0001). The values are presented as means ± SD (n = 5/group).

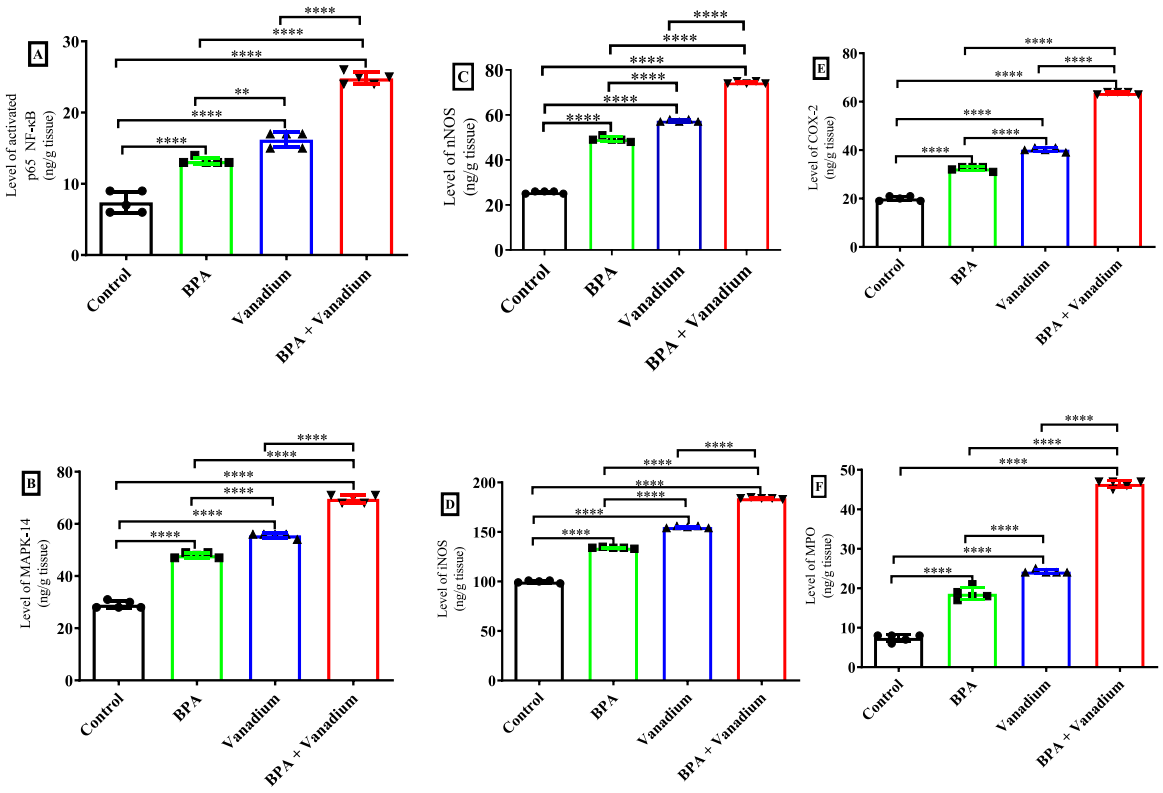

Fig. 4. The effect of BPA and/or vanadium on the levels of inflammatory and pro-inflammatory cytokines in the prefrontal cortex of the mice. (A) level of NF-κB, (B) level of MAPK-14, (C) level of nNOS, (D) level of iNOS; (E) level of COX-2, and (F) level of MPO. The data obtained was analyzed using one-way ANOVA (**P < 0.01, ****P < 0.0001). The values are presented as means ± SD (n = 5/group).

Effect of bisphenol A, vanadium, and their combination on the levels of neurotransmitters in the prefrontal cortex

The study examined how BPA, vanadium, and a combination of both affect the levels of acetylcholinesterase (AChE), serotonin, and dopamine in the prefrontal cortex of mice (Fig. 6A-C). The results showed that exposure to BPA, vanadium, and the mixture of both significantly lowered the levels of AChE compared with the control ($F(3, 16) = 2359$, $p < 0.0001$, Fig. 6A). On the other hand, compared with the control group, the levels of serotonin in the prefrontal cortex of the mice exposed to BPA, vanadium, and BPA + vanadium co-exposed were significantly downregulated ($F(3, 16) = 6713$, $p < 0.0001$, Fig. 6B). Furthermore, we observed that the levels of dopamine were significantly reduced in the prefrontal cortex of the mice exposed to BPA, vanadium, and BPA + vanadium co-exposed compared with the control ($F(3, 16) = 14297$, $p < 0.0001$, Fig. 6C). These results suggest that BPA, vanadium, and their combination disrupt the normal function of these key neurotransmitters in the prefrontal cortex of the mice.

Effect of bisphenol A, vanadium, and their combination on the histopathological observations in the prefrontal cortex (Fig. 7)

In the control group, the H&E-stained sections of the prefrontal cortex of the mice showed the normal appearing neurons (yellow arrows). However, there was a heterogeneous appearance of neuronal swelling and vacuolation in the sections of the mice exposed to BPA, vanadium, and BPA + vanadium decoction. Additionally, shrunken eosinophilic neurons with features of pyknotic or karyorrhectic nuclei (red arrows) were observed.

The Golgi impregnation technique allows for a detailed and clear visualization of both the intricate arborization patterns of apical and basal dendrites, as well as the spines present on them. The dendritic structures of cortical excitatory neurons are distinctly identifiable by the presence of spines. In the Golgi-stained sections, the prefrontal cortices of the control group mice showed dendritic arborization of the neurons with apical (double yellow arrows) and basal (double blue arrows) dendrites. The dendrites exhibited significant length and a complex intertwining pattern with those of adjacent neurons, creating a dense network of connections. In contrast, the dendritic morphology observed in the BPA-treated, vanadium-exposed, and BPA + vanadium co-treated groups showed marked alterations. Specifically, these groups displayed considerably shorter dendrites with reduced or scanty arborization. The dendrites (double red arrows) were thinner and slender and are significantly fewer in number or absent in the regions imaged from layers II-III of the prefrontal cortex in these experimental groups. These qualitative observations align with quantitative measurements, indicating a substantial reduction in the mean (±SD) length of basal dendrites among the BPA, vanadium, and BPA + vanadium cohorts. The statistical analysis confirmed this finding as highly significant, with the mean lengths markedly differing when compared to the control group ($F(3, 16) = 586918$, $p < 0.0001$, Fig. 8).

Discussion

Several studies have shown that exposure to BPA or vanadium can impair learning and memory (Rebuli et al., 2015; Audu et al., 2020; Nayan et al., 2022). The prefrontal cortex, which plays a key role in these functions, is vulnerable to deleterious modifications from noxious environmental factors like BPA and vanadium. In our experiment, mice were exposed to BPA, vanadium, or both showed lower movement and exploration compared to mice that were not exposed. The control mice displayed normal levels of activity and exploration. Additionally, the exposed groups had higher anxiety levels during the open-field tests compared to the control group. Specifically, the BPA + vanadium co-treated group exhibited significantly more pronounced reductions in exploration and locomotor activities, as well as higher anxiety levels,

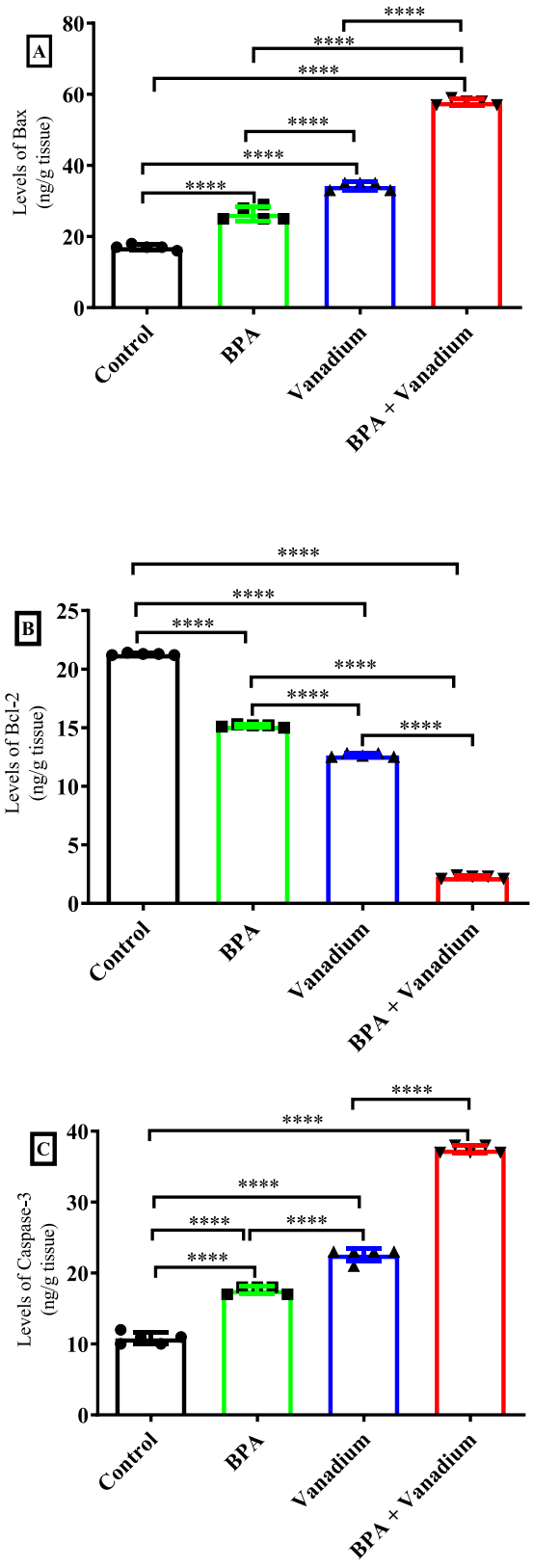

Fig. 5. The effect of BPA and/or vanadium on the levels of apoptotic and pro-apoptotic markers in the prefrontal cortex of mice. (**A**) level of Bax, (**B**) level of Bcl-2, and (**C**) level of caspase-3. The data obtained was analyzed using one-way ANOVA (****P < 0.0001). The values are presented as means ± SD (n = 5/group).

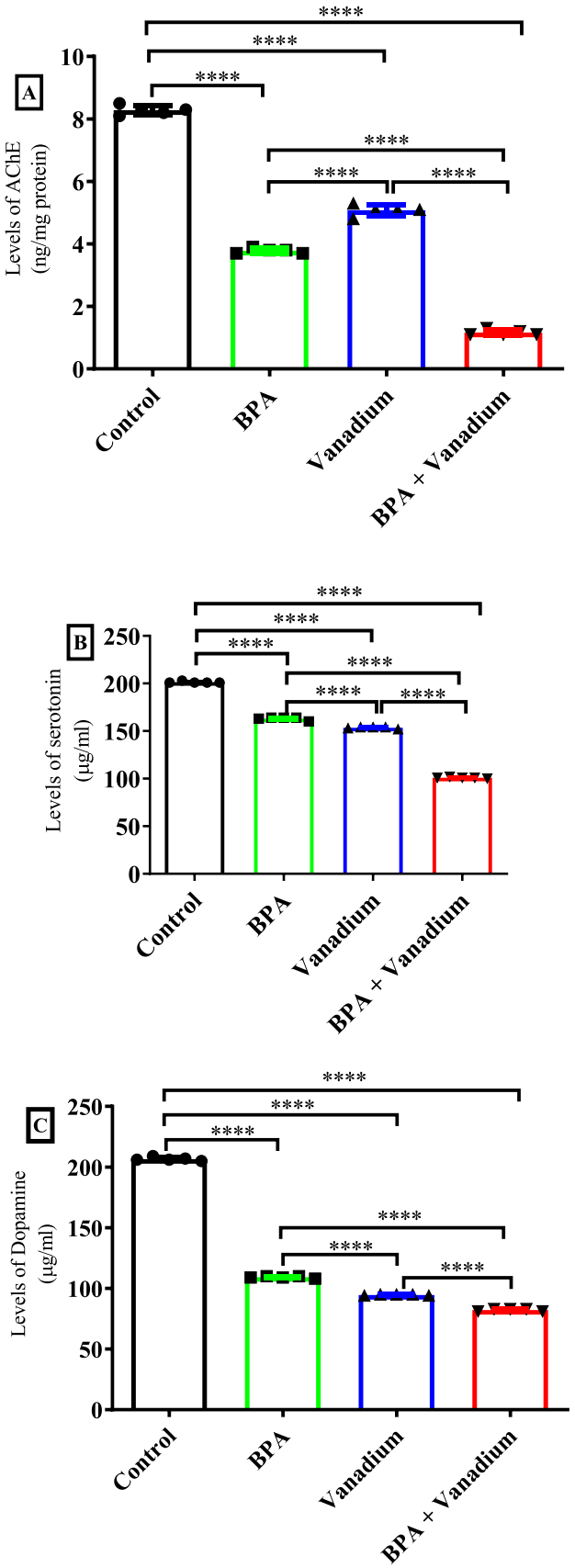

Fig. 6. The effect of BPA and/or vanadium on the levels of neurotransmitters in the prefrontal cortex of the mice. (A) level of AChE, (B) level of Serotonin, and (C) level of Dopamine. The data obtained was analyzed using one-way ANOVA (***P < 0.0001). The values are presented as means ± SD (n = 5/group).

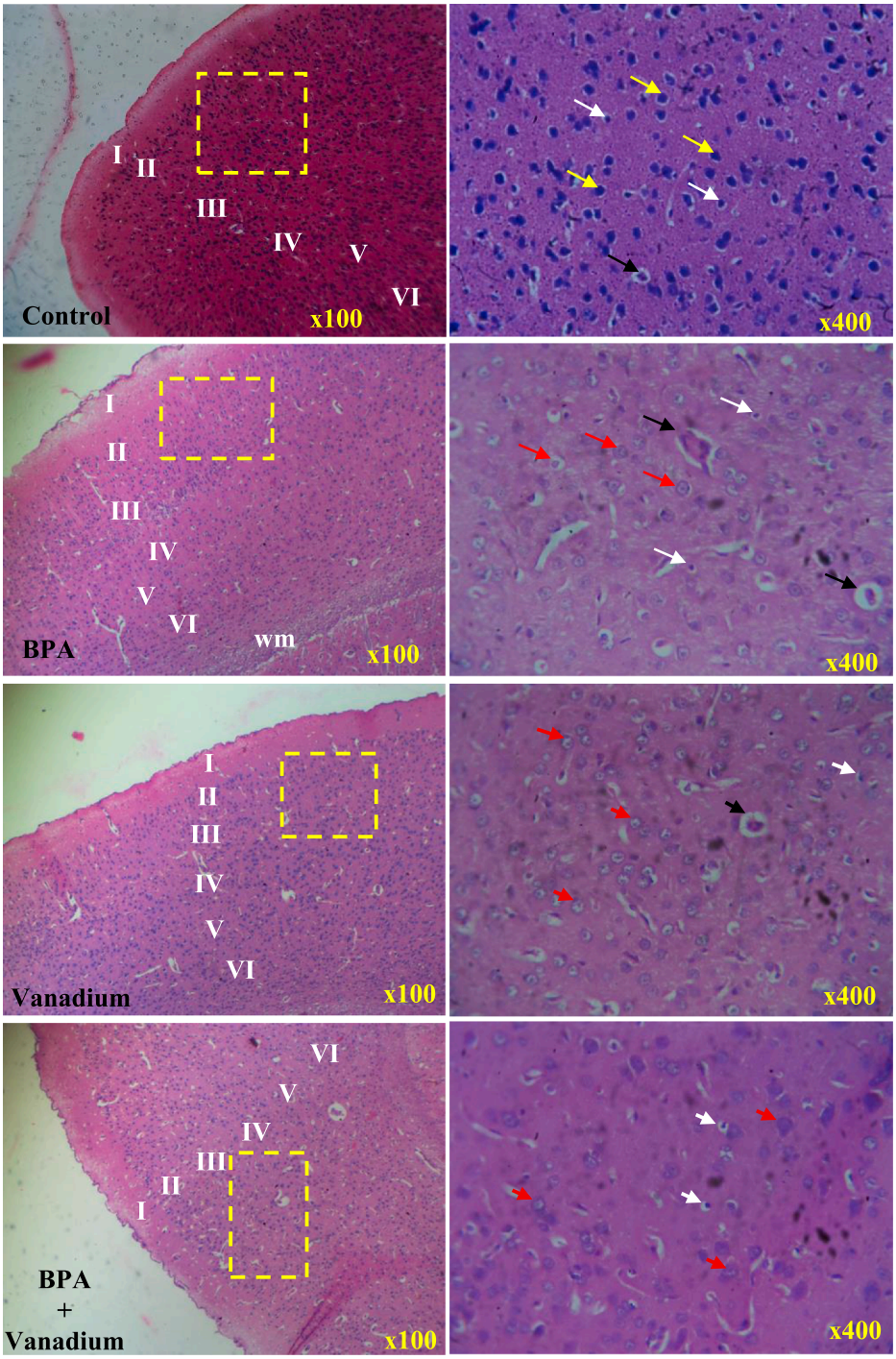

Fig. 7. a: Representative photomicrographs of the H&E-stained sections of the prefrontal cortices of the experimental mice. The neuroarchitecture organization of the prefrontal cortex, from superficial to deep: molecular layer (I), external granular layer (II), external pyramidal layer (III), internal granular layer (IV), internal pyramidal layer (V), and polymorphic layer (VI) bordered by the cerebral white matter (wm). Adjacent to each of the photomicrographs are the respective higher magnifications of the upper squared area in layers II and III. Within the sections are neuronal cell bodies with intact cytoplasm (yellow arrows), degenerating neurons (red arrows), well-demarcated and deeply stained neuroglial cells (white arrowheads), and normal blood vessels (black arrowheads) within the neuropil. Fig. 7b: The effect of BPA and/or vanadium on the percentage of degenerating neurons in the prefrontal cortices of the experimental mice. The data obtained was analyzed using one-way ANOVA (****$p < 0.0001$). Data is expressed as mean ± SD ($n = 5$ mice/group). Fig. 7c: Photomicrograph of the Golgi-stained neurons in the prefrontal cortex of the representative mice in the control group displayed structural preservation with well-defined cell bodies, extended dendritic trees (double yellow and blue arrow heads), strong contrast, and clearly defined intact dendritic arbors with dendritic spines. The neurons in the prefrontal cortex of the representative mice in the BPA-treated, vanadium-treated, and the BPA and vanadium co-treated groups, respectively, exhibited impaired soma delineation and reduced dendritic staining, along with compromised dendritic tree arborizations (yellow asterisks). The loss of most dendritic spines was particularly evident in the BPA-treated and the BPA + vanadium co-treated groups. The white arrow is showing the regularly attached pia mater. Fig. 7d: The effect of BPA and/or vanadium on the basal dendrite length. The data obtained was analyzed using one-way ANOVA (****$p < 0.0001$). Data is expressed as mean ± SD ($n = 5$ mice/group).

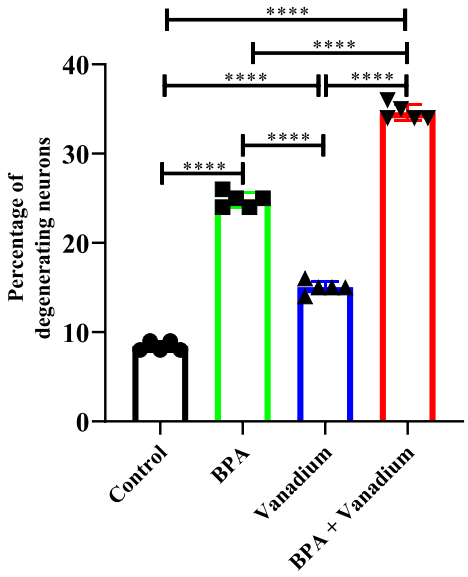

Fig. 7. (*continued*).

compared to the groups treated with either BPA or vanadium alone. Similarly, findings from the elevated plus maze test aligned with those of the open-field tests, revealing a strong anxiogenic response in the mice exposed to BPA, vanadium, and the BPA + vanadium combination when compared to the control group. The result of the behavioral assay disagrees with the result of Rebuli et al. (2015), who reported that no consistent effect of BPA was seen at the endpoint. Contrary to that, our study agrees with the report of the study of Wang et al. (2020), who reported that exposure to BPA triggered anxiety and depression-like behavior in the experimental animals. Similarly, result of our study disagrees with the report of Dyer and De Butte (2022), who reported that exposure to vanadium did not affect exploration, locomotion, or anxiety-like behavior in the open field test. Conversely to that, our study agrees with the report of Domingo (1996) and Soazo and Garcia (2007). Olopade et al. (2011) attributed this modulatory behavioral observation to vanadium-induced muscular weakness. The variance in these observations may be connected to the difference in duration of exposure. We therefore propose that the behavioral deficits associated with BPA and vanadium, and the aggravated behavioral deficits seen in the BPA + vanadium co-treated groups, as observed in this study, may partly result from the neurotoxic effects of these xenobiotics on the prefrontal cortex, with corresponding up-regulated conflicting modulation of neurotransmitters in the synaptic cleft due to altered reuptake or compromised activities.

The excessive production of reactive oxygen species (ROS), triggered by exposure to various environmental contaminants, leads to the oxidation of polyunsaturated fatty acids in cellular phospholipids. This process generates harmful by-products such as 4-hydroxynonenal and malondialdehyde (MDA), which serve as biomarkers of lipid peroxidation, a crucial indicator of oxidative stress within cells. To combat such oxidative damage, the body relies on a network of endogenous antioxidants, including superoxide dismutase (SOD), catalase (CAT), glutathione peroxidase (GPx), glutathione-S-transferase (GST), and reduced glutathione (GSH). These antioxidants are vital for the direct elimination of reactive oxygen species, thus providing a defense mechanism against cellular oxidative harm (Afzal et al., 2023). In a study by Khan et al. (2026), it was reported that mice exposed to BPA had significantly decreased levels of antioxidant enzymes in their cerebellar cortex. This reduction indicates an inhibition of the antioxidant defense system, which may lead to the accumulation of neurotoxic radicals in the brain tissue. As observed in this study, this observation points to the adverse effects of exposure to BPA and vanadium, which resulted in increased generation of reactive oxygen species, ultimately overwhelming the physiological antioxidant defenses and contributing to oxidative damage in the prefrontal cortex. The metabolites resulting from reactive oxygen species have the potential to act as cytotoxic agents, inflicting substantial oxidative damage that compromises the normal functioning of key biomolecules, which include lipids integral to cell membranes, as well as DNA and proteins essential for cellular integrity (Juan et al., 2021). This extensive damage may help elucidate the significant decline in the levels of vital antioxidants such as superoxide dismutase, catalase, glutathione peroxidase, and glutathione. This decline coincides with a significant increase in malondialdehyde levels, arising from the exposure to BPA, vanadium, and their combination, as depicted in Fig. 3A-E. This result was in accordance with various studies, which demonstrated that upon exposure to BPA or vanadium, there is an increased generation of ROS and a decreased endogenous antioxidant in the brain.

Our study found that exposure to BPA, vanadium, and the combination of BPA + vanadium significantly stimulates inflammation and pro-inflammatory processes by activating several key pathways, including activated p65 NF-kB, MAPK-14, iNOS, nNOS, COX-2, and MPO (Fig. 4A-F). We observed a strong interaction between activated p65 NF-kB and the increased levels of MAPK-14, iNOS, nNOS, COX-2, and MPO in the prefrontal cortex of mice treated with BPA, those exposed to vanadium, and those co-treated with both substances, compared to the control group. Several studies have indicated that pro-inflammatory cytokines are crucial in modulating the immune response in inflammatory disorders and are closely associated with inflammatory processes (Chen et al., 2017; Kany et al., 2019; Bhol et al., 2024). The production and interactions of inflammatory and pro-inflammatory cytokines contribute to neuroinflammation and may stimulate detrimental processes in the brain, thereby compromising its neurophysiological functions (Moens et al., 2013). The elevated levels of activated p65 NF-kB, MAPK-14, iNOS, nNOS, COX-2, and MPO may be linked to increased inflammation and tissue damage resulting from exposures to BPA, vanadium, and their combined effects. Our findings align with those of Adedara et al. (2020), who reported that exposure to water-borne nickel resulted in a significant increase in the activities of inflammatory and pro-inflammatory cytokines in the cerebrum, cerebellum, and liver of the exposed rats, indicating induction of neuro-hepatic inflammation. Consequently, we suggest that inhibiting the activation of p65 NF-kB, MAPK-14, iNOS, nNOS, COX-2, and MPO could represent a promising therapeutic target for mitigating the

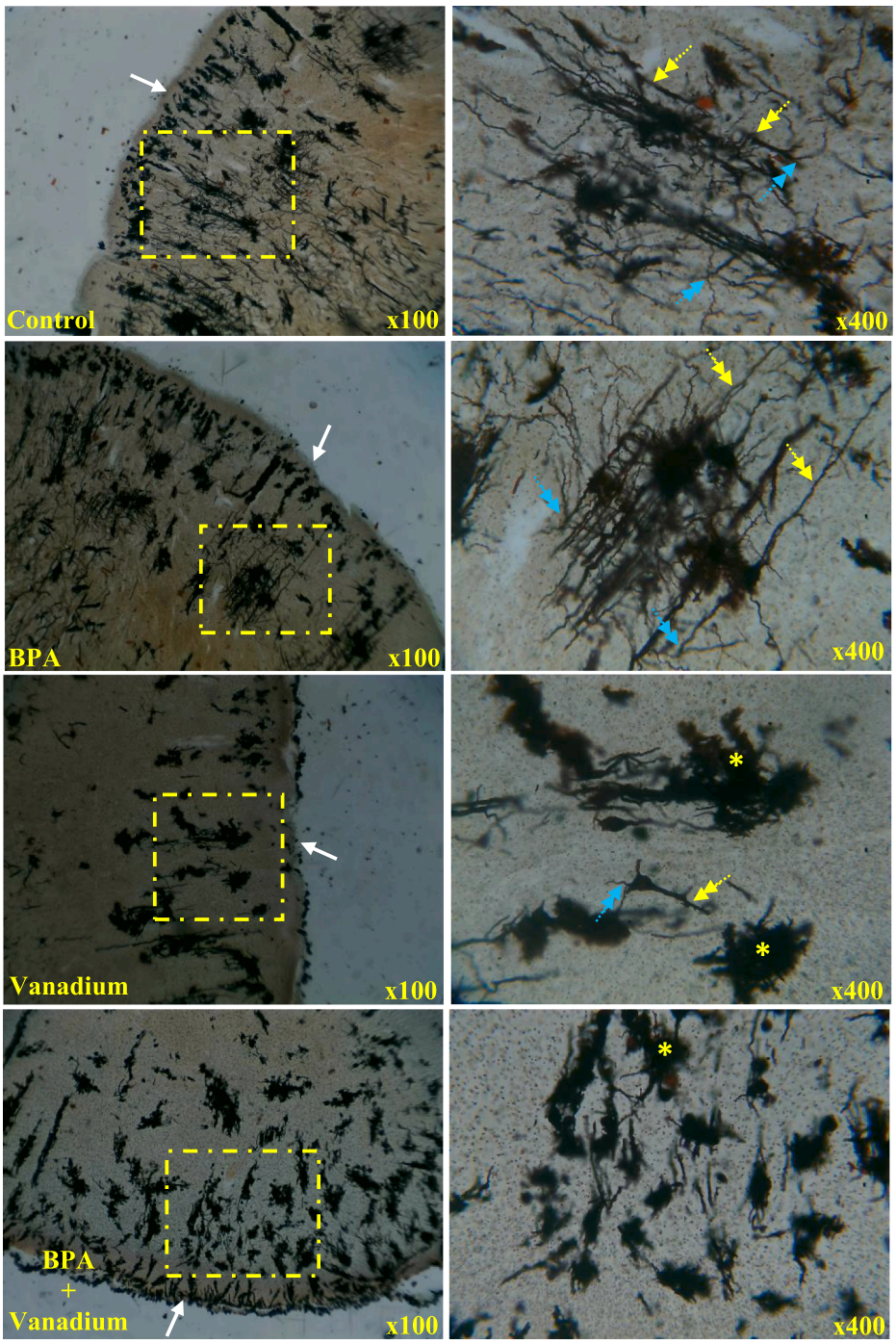

Fig. 7. (*continued*).

harmful effects of BPA and vanadium on the brain.

Previous research has established a compelling link between oxidative stress induced by transition metals and the activation of various neuronal apoptotic proteins, ultimately resulting in the death of neuronal cells (López et al., 2006; Khan et al., 2019a, 2019a). One of the pivotal events in this apoptotic process is the translocation of the pro-apoptotic protein Bax from the cytosol to the mitochondria. This movement serves as a critical trigger for mitochondrial-dependent apoptosis, marked by a series of biological changes including the release of cytochrome *c*, onset of mitochondrial dysfunction, and the subsequent activation of caspases. These events together culminate in irreversible cell death (Putcha et al., 1999; Kirkland and Franklin, 2003; Adesso et al., 2018). In numerous neuronal disorders, an increased activation of Bax has been noted alongside a suppression of the anti-apoptotic protein Bcl-2. This imbalance forms a crucial aspect of understanding how the ratio of pro-apoptotic to anti-apoptotic proteins can profoundly influence the fate of neurons following exposure to toxic stimuli. When brain tissue is subjected to transition metal exposure, activated Bax upregulates caspase-9, which in turn leads to the cleavage and activation of caspase-3. This pathway is recognized as a vital mediator of the apoptotic process (Anilkumar and Prehn, 2014; Mahdavi et al., 2018). Moreover, Bcl-2 plays a significant role as a survival factor within the intrinsic apoptotic pathway. It helps to inhibit the nuclear translocation of factors that initiate apoptosis and prevents the cleavage of caspases. Among these, caspase-3 is particularly important; its activation is synonymous with neuronal cell death and is a hallmark feature

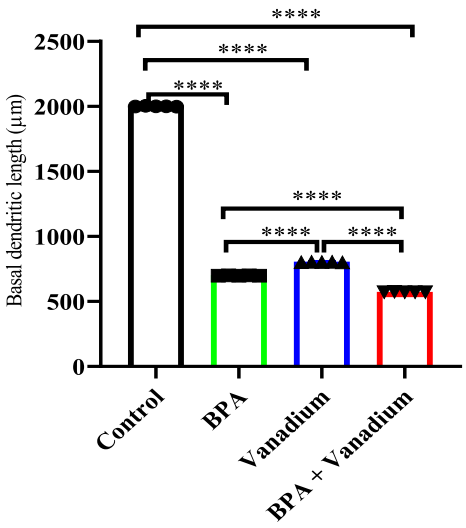

Fig. 7. (*continued*).

of a range of neurodegenerative diseases and disorders (Namura et al., 1998; Li and Yuan, 2008; Ojala and Sutinen, 2017). The activation of caspase-3 leads to the cleavage of poly (ADP-ribose) polymerase-1 (PARP-1), a protein essential for DNA repair, which results in energy deprivation in cells and ultimately triggers apoptotic cell death (Sairanen et al., 2009; Chaitanya et al., 2010; Chen et al., 2019). In light of these mechanisms, the present study reveals that exposure to BPA, vanadium, and their combination precipitates a notable increase in the levels of both Bax and caspase-3, while simultaneously reducing the levels of Bcl-2 (Fig. 5A-C). The observed elevation in Bax and caspase-3, coupled with the diminished Bcl-2 levels across groups treated with BPA, vanadium, and the combined treatment of both substances, strongly indicates the activation of neuronal apoptotic pathways. These findings align with previous studies that have implicated Bax, caspase-3, and Bcl-2-dependent cascades in the apoptosis induced by transition metals across various tissues (Kim and Sharma, 2006; Zwolak, 2020).

Alterations in biomarkers of neurotoxicity, such as AChE, serotonin, and dopamine, have been used to assess the neurotoxicity of environmental chemicals (Liu et al., 2024). AChE serves as a robust and reliable diagnostic and prognostic marker for neurotoxicity and neuroinflammation (Mucci et al., 2020). Our results indicated a decrease in AChE, serotonin, and dopamine levels in the groups treated with bisphenol A, vanadium, and the combination of BPA and vanadium, compared to the control group (Fig. 6A-C). The observed reductions in AChE, serotonin, and dopamine levels may suggest the neurotoxic effects of BPA, vanadium, and their combination at the doses administered. These decreases may result from the inhibitory effects of BPA, vanadium, and the combination of both substances on the metabolic pathways related to AChE, serotonin, and dopamine. Our findings are consistent with previous studies by Bansal et al. (2017) and Susiarjo et al. (2017), which reported decreased levels of monoamine neurotransmitters in the hippocampus of rodents exposed to BPA. Additionally, Sharma et al. (1986) observed reductions in serotonin and dopamine levels in the hippocampus of rodents exposed to vanadium. In our study, the most significant decreases in acetylcholinesterase (AChE), serotonin, and dopamine levels were found in the prefrontal cortex of mice that were co-exposed to both BPA and vanadium. This suggests a neurotoxic synergistic effect of these two xenobiotics on the prefrontal cortex.

Histological study in the prefrontal cortex revealed diverse neurodiagnostic features (Fig. 7a, 7b, 7c, and 7d). In the control group, the H&E-stained sections of the prefrontal cortex showed normal pyramidal neurons (indicated by yellow arrows). In contrast, the sections from mice exposed to BPA, vanadium, and a combination of BPA and vanadium decoction exhibited a diverse range of neuronal swelling and vacuolation. Additionally, shrunken eosinophilic neurons displaying characteristics of pyknotic or karyorrhectic nuclei were observed (indicated by red arrows). In the Golgi-stained sections, the prefrontal cortices of the control group mice exhibited healthy dendritic arborization in the pyramidal neurons, indicated by white arrows.

Changes in the morphological patterns of dendrites are particularly significant, as researchers have proposed that the apical and basal dendritic structures may serve as distinct zones for various classes of synaptic inputs. Notably, the spines located on these dendrites are highly susceptible to pathological events, exhibiting an exponential increase in vulnerability (Kang et al., 2015; Barón-Mendoza et al., 2021). These dendritic spines function as the primary sites for excitatory inputs mediated by glutamate within the pyramidal neurons of the cerebral cortex (Kasai, 2023). The importance of these spines extends beyond mere connectivity; they act as critical biochemical microenvironments. They are involved in a range of processes that enhance synaptic plasticity and energy transfer, essentially invigorating the dendritic architecture (Moore et al., 2025; Schünemann et al., 2025). Pathological alterations observed within the cerebral cortex are hypothesized to stem from mechanical injury, which can be exacerbated by neurotoxic agents. This initial damage is followed by a cascade of secondary effects, including heightened neuronal cell death, inflammatory responses, and oxidative stress, ultimately contributing to further degeneration of neuro-cortical structures (Kweon et al., 2017; Castejón, 2019). This observation is consistent with the reduction of the dendritic processes as shown in our study by Golgi staining (Fig. 7**c**) and supports the notion that impaired dendritic branching and spine formation can result from exposure to BPA (Li et al., 2025) or vanadium (Ladagu et al., 2023).

Conclusion

In conclusion, the findings from this study indicate that exposure to BPA and vanadium may result in deleterious effects on the brain health of mice, primarily due to the combined impact of these substances. This situation raises significant concerns regarding human exposure to BPA and vanadium, especially considering their prevalent use across numerous industries, their presence in food processing materials, and the potential consumption of untreated underground water, which could contain these hazardous substances. Moreover, the data obtained in this research reveal that both BPA and vanadium tend to accumulate in the prefrontal cortex of the experimental mice. This accumulation appears to disrupt the normal functioning of the prefrontal cortex, leading to a range of neurological abnormalities that have been observed in the

affected mice. The implications of these findings highlight the need for further investigation into the neurologic risks associated with these compounds and their potential effects on the functional integrity of the brain and its related topographies.

Compliance with ethical standards

This study was conducted in strict compliance with all applicable international, national, and institutional regulations regarding the ethical treatment, care, and use of laboratory animals in research. We ensure full compliance with the ARRIVE (Animals in Research: Reporting In Vivo Experiments) Guidelines, which provide a framework for the responsible and humane use of animals in research.

Funding

No grant or funding was received for this study.

Conflicts of Interest

The authors report there are no competing interests to declare.

Data availability

The data supporting this study's findings can be accessed upon request by contacting the corresponding author, who will provide the necessary details and support for your inquiry.

References

Abd Elkader, H.A.E., Al-Shami, A.S., 2023. Chronic exposure to bisphenol A induces behavioural, neurochemical, histological, and ultrastructural alterations in the ganglia tissue of the date mussels Lithophaga lithophaga. Environ. Sci. Pollut. Res. Int. 30 (50), 109041–109062. https://doi.org/10.1007/s11356-023-29853-3.

Adedara, I.A., Adegbosin, A.N., Abiola, M.A., Odunewu, A.A., Owoeye, O., Owumi, S.E., et al., 2020. Neurobehavioural and biochemical responses associated with exposure to binary waterborne mixtures of zinc and nickel in rats. Environ. Toxicol. Pharmacol. 73, 103294. https://doi.org/10.1016/j.etap.2019.103294.

Adelakun, S.A., Ogunlade, B., Aniah, J.A., Akwu, B.P., Afolabi, M.O., 2024. Excessive caffeine intake inhibits steroidogenesis, folliculogenesis and disrupts utero-ovarian tissue histomorphology integrity in experimental rats, and precipitates polycystic ovary syndrome in Sprague-Dawley rats. Food Chem. Adv. 4, 100678. https://doi.org/10.1016/j.focha.2024.100678.

Adesso, S., Paterniti, I., Cuzzocrea, S., Fujioka, M., Autore, G., Magnus, T., et al., 2018. AST-120 reduces neuroinflammation induced by indoxyl sulfate in glial cells. J. Clin. Med. 7, 365. https://doi.org/10.3390/jcm7100365.

Afzal, S., Abdul Manap, A.S., Attiq, A., Albokhadaim, I., Kandeel, M., Alhojaily, S.M., 2023. From imbalance to impairment: the central role of reactive oxygen species in oxidative stress-induced disorders and therapeutic exploration. Front. Pharmacol. 14, 1269581. https://doi.org/10.3389/fphar.2023.1269581.

Amaral, L.M.P.F., Moniz, T., Silva, A.M.N., Rangel, M., 2023. Vanadium compounds with antidiabetic potential. Int. J. Mol. Sci. 24 (21), 15675. https://doi.org/10.3390/ijms242115675.

Anilkumar, U., Prehn, J.H., 2014. Anti-apoptotic BCL-2 family proteins in acute neural injury. Front. Cell Neurosci. 8, 281. https://doi.org/10.3389/fncel.2014.00281.

Audu, R.S., Olopade, F.E., Ladagu, A.D., Hassan, S.U., Yahaya, A., Olopade, J.O., 2020. Behavioral and histomorphological changes in the developing brains of vanadium-exposed mice pups: protective role of minocycline. Arch. Bas Appl. Med 8, 95–102.

Aureliano, M., De Sousa-Coelho, A.L., Dolan, C.C., Roess, D.A., Crans, D.C., 2023. Biological consequences of vanadium effects on formation of reactive oxygen species and lipid peroxidation. Int. J. Mol. Sci. 24 (6), 5382. https://doi.org/10.3390/ijms24065382.

Avila-Costa, M.R., Fortoul, T.I., Niño-Cabrera, G., Colín-Barenque, L., Bizarro-Nevares, P., Gutiérrez-Valdez, A.L., et al., 2006. Hippocampal cell alterations induced by the inhalation of vanadium pentoxide (V_2O_5) promote memory deterioration. Neurotoxicology 7 (6), 1007–1012.

Azami, K., Tabrizian, K., Hosseini, R., Seyedabadi, M., Shariatpanahi, M., Noorbakhsh, F., et al., 2012. Nicotine attenuates spatial learning deficits induced by sodium metavanadate. Neurotoxicology 33 (1), 44–52.

Balabanic, D., Filipic, M., Krivograd Klemencic, A., et al., 2021. Genotoxic activity of endocrine disrupting compounds commonly present in paper mill effluents. Sci. Total Environ. 794, 148489.

Banaderakhshan, R., Kemp, P., Breul, L., Steinbichl, P., Hartmann, C., Fürhacker, M., 2022. Bisphenol A and its alternatives in Austrian thermal paper receipts, and the migration from reusable plastic drinking bottles into water and artificial saliva using UHPLC-MS/MS. Chemosphere 286, 131842.

Bancroft, J.D., Gamble, M., 2008. Theory and practice of histological techniques, 6th edn. Churchill Livingstone, London.

Bansal, A., Rashid, C., Xin, F., Li, C., Polyak, E., Duemler, A., et al., 2017. Sex- and dose-specific effects of maternal bisphenol A exposure on pancreatic islets of first- and second-generation adult mice offspring. Environ. Health Perspect. 125 (9), 097022. https://doi.org/10.1289/EHP1674.

Baralić, K., Jorgovanović, D., Živančević, K., Djordjević, A.B., Miljaković, E.A., Miljković, M., Kotur-Stevuljević, J., Antonijević, B., Đukić-Ćosić, D., 2021. Combining in vivo pathohistological and redox status analysis with in silico toxicogenomic study to explore the phthalates and bisphenol A mixture-induced testicular toxicity. Chemosphere 267, 129296. https://doi.org/10.1016/j.chemosphere.2020.129296.

Bradley, A.E., Bolon, B., Butt, M.T., Cramer, S.D., Czasch, S., Garman, R.H., et al., 2020. Proliferative and nonproliferative lesions of the rat and mouse central and peripheral nervous systems: new and revised INHAND terms. Toxicol. Pathol. 48 (7), 827–844. https://doi.org/10.1177/0192623320951154.

Bansal, A.S., Seton, K.A., Brooks, J.C.W., Carding, S.R., 2025. Cognitive dysfunction in myalgic encephalomyelitis/chronic fatigue syndrome—aetiology and potential treatments. Int. J. Mol. Sci. 26 (5), 1896. https://doi.org/10.3390/ijms26051896.

Barceloux, D.G., 1999. Vanadium. J. Toxicol. Clin. Toxicol. 37 (2), 265–278. https://doi.org/10.1081/clt-100102425—erratum. J Toxicol Clin Toxicol 2000;38(7):813.

Barón-Mendoza, I., Maqueda-Martínez, E., Martínez-Marcial, M., De la Fuente-Granada, M., Gómez-Chavarin, M., González-Arenas, A., 2021. Changes in the number and morphology of dendritic spines in the hippocampus and prefrontal cortex of the C58/J mouse model of autism. Front. Cell. Neurosci. 15, 726501. https://doi.org/10.3389/fncel.2021.726501.

Ben-Azu, B., Aderibigbe, A.O., Omogbiya, I.A., Ajayi, A.M., Owoeye, O., Olonode, E.T., et al., 2018. Probable mechanisms involved in the antipsychotic-like activity of morin in mice. Biomed. Pharm. 105, 1079–1090. https://doi.org/10.1016/j.biopha.2018.06.057.

Beutler, E., Duron, O., Kelly, B.M., 1963. Improved method for the determination of blood glutathione. J. Lab Clin. Med. 61, 882–888.

Bhol, N.K., Bhanjadeo, M.M., Singh, A.K., Dash, U.C., Ojha, R.R., Majhi, S., et al., 2024. The interplay between cytokines, inflammation, and antioxidants: mechanistic insights and therapeutic potentials of various antioxidants and anti-cytokine compounds. Biomed. Pharm. 178, 117177. https://doi.org/10.1016/j.biopha.2024.117177.

Bradford, M.M., 1976. A rapid and sensitive method for the quantitation of microgram quantities of protein utilizing the principle of protein-dye binding. Anal. Biochem. 72, 48–54. https://doi.org/10.1016/0003-2697(76)90527-3.

Brown, T.J., Idoine, N.E., Raycraft, E.R., Hobbs, S.F., Shaw, R.A., Everett, P., et al., 2019. World Min. Prod. 2013–2017.

Caballero-Casero, N., Lunar, L., Rubio, S., 2016. Analytical methods for the determination of mixtures of bisphenols and derivatives in human and environmental exposure sources and biological fluids. A review. Anal. Chim. Acta 908, 22–53.

Castejón, O.J., 2019. Morphopathological changes of dendrites in experimental animals and in human nervous diseases. J. Neurol. Stroke 9 (2), 98–104. https://doi.org/10.15406/jnsk.2019.09.00356.

Chaitanya, G.V., Steven, A.J., Babu, P.P., 2010. PARP-1 cleavage fragments: signatures of cell-death proteases in neurodegeneration. Cell Commun. Signal 8, 31. https://doi.org/10.1186/1478-811X-8-31.

Chen, L., Deng, H., Cui, H., Fang, J., Zuo, Z., Deng, J., Li, Y., Wang, X., Zhao, L., 2017. Inflammatory responses and inflammation-associated diseases in organs. Oncotarget 9 (6), 7204–7218. https://doi.org/10.18632/oncotarget.23208.

Chen, P., Yang, J., Xiao, B., Zhang, Y., Liu, S., Zhu, L., 2021. Mechanisms for the impacts of graphene oxide on the developmental toxicity and endocrine disruption induced by bisphenol A on zebrafish larvae. J. Hazard. Mater. 408, 124867.

Chen, Y.H., Fu, Y.C., Wu, M.J., 2019. Does resveratrol play a role in decreasing the inflammation associated with contrast induced nephropathy in rat model? J. Clin. Med 8, 147.

Chin-Chan, M., Navarro-Yepes, J., Quintanilla-Vega, B., 2015. Environmental pollutants as risk factors for neurodegenerative disorders: Alzheimer and Parkinson diseases. Front. Cell Neurosci. 9, 124.

Clancy, H.A., Sun, H., Passantino, L., Kluz, T., Muñoz, A., Zavadil, J., Costa, M., 2012. Gene expression changes in human lung cells exposed to arsenic, chromium, nickel or vanadium indicate the first steps in cancer. Metallomics 4 (8), 784–793.

Correa, M., Sanchis-Segura, C., Aragon, C.M., 2001. Brain catalase activity is highly correlated with ethanol-induced locomotor activity in mice. Physiol. Behav. 73 (4), 641–647.

Cui, L., Li, S., Wang, S., Wu, X., Liu, Y., Yu, W., et al., 2024. Major depressive disorder: hypothesis, mechanism, prevention and treatment. Signal Transduct. Target Ther. 9 (1), 30.

Dagher, J.B., Hahn-Townsend, C.K., Kaimal, A., Al Mansi, M., Henriquez, J.E., Tran, D. G., Laurent, C.R., Bacak, C.J., Buechter, H.E., Cambric, C., et al., 2021. Independent and combined effects of Bisphenol A and Diethylhexyl Phthalate on gestational outcomes and offspring development in Sprague-Dawley rats. Chemosphere 263, 128307. https://doi.org/10.1016/j.chemosphere.2020.128307.

Dayanand, Y., Pather, R., Xulu, N., Booysen, I., Sibiya, N., Khathi, A., Ngubane, P., 2024. Exploring the biological effects of anti-diabetic vanadium compounds in the liver, heart and brain. Diabetes Metab. Syndr. Obes. 17, 3267–3278.

Domingo, L., 1996. Vanadium: A review of the reproductive and developmental toxicity. Reprod. Toxicol. 10 (3), 175–182. https://doi.org/10.1016/0890-6238(96)00019-6.

Duffus, J.H., 2002. Heavy metals –A meaningless term? Pure Appl. Chem. 4, 793–807.

Durovcova, I., Spackova, J., Puskar, M., Galova, E., Sevcovicova, A., 2018. Bisphenol A as an environmental pollutant with dual genotoxic and DNA-protective effects. Neuro Endocrinol. Lett. 9, 294–298.
Dyer, A., De Butte, M., 2022. Neurobehavioral effects of chronic low-dose vanadium administration in young male rats. Behav. Brain Res. 419, 113701. https://doi.org/10.1016/j.bbr.2021.113701.
Ellman, G.L., Courtney, K.D., Andres, V., Jr, Feather-Stone, R.M., 1961. A new and rapid colorimetric determination of acetylcholinesterase activity. Biochem. Pharm. 7, 88–95.
Fatola, O.I., Olaolorun, F.A., Olopade, F.E., Olopade, J.O., 2019. Trends in vanadium neurotoxicity. Brain Res. Bull. 145, 75–80.
Femi-Akinlosotu, O.M., Shokunbi, M.T., Naicker, T., 2019. Dendritic and synaptic degeneration in pyramidal neurons of the sensorimotor cortex in neonatal mice with kaolin-induced hydrocephalus. Front. Neuroanat. 13, 38.
Folarin, O., Olopade, F., Onwuka, S., Olopade, J., 2016. Memory deficit recovery after chronic vanadium exposure in mice. Oxid. Med. Cell. Longev. 2016 (1), 4860582.
Fu, J.J., Guo, Y.Y., Yang, L.H., Han, J., Zhou, B.S., 2020. Nano-TiO2 enhanced bioaccumulation and developmental neurotoxicity of bisphenol a in zebrafish larvae. Environ. Res. 187, 109682. https://doi.org/10.1016/j.envres.2020.109682.
Funahashi, S., 2017. Working memory in the prefrontal cortex. Brain Sci. 7 (5), 49.
Gambino, D., 2011. Potentiality of vanadium compounds as anti-parasitic agents. Coord. Chem. Rev. 255, 2193–2203.
Ge, C., Wang, S., Wu, X., Lei, L., 2023. Quercetin mitigates depression-like behavior via the suppression of neuroinflammation and oxidative damage in corticosterone-induced mice. J. Chem. Neuroanat. 132, 102313.
Geens, T., Aerts, D., Berthot, C., Bourguignon, J.P., Goeyens, L., Lecomte, P., et al., 2012. A review of dietary and non-dietary exposure to bisphenol-A. Food Chem. Toxicol. 50 (10), 3725–3740.
Gowder, S.J., 2013. Nephrotoxicity of bisphenol A (BPA)—An updated review. Curr. Mol. Pharmacol. 6, 163–172. https://doi.org/10.2174/1874467207666140410115823.
Guo, J.Q., Wu, C.H., Zhang, J.M., Qi, X.J., Lv, S.L., Jiang, S., Zhou, T., Lu, D.S., Feng, C., Chang, X.L., et al., 2020. Prenatal exposure to mixture of heavy metals, pesticides and phenols and IQ in children at 7 years of age: The SMBCS study. Environ. Int. 139, 105692. https://doi.org/10.1016/j.envint.2020.105692.
Habib, H.M., Ibrahim, W.H., 2011. Nutritional quality of 18 date fruit varieties. Int. J. Food Sci. Nutr. 62 (5), 544–551.
He, Z., Han, S., Zhu, H., Hu, X., Li, X., Hou, C., et al., 2020. The protective effect of vanadium on cognitive impairment and the neuropathology of Alzheimer's disease in APPSwe/PS1dE9 mice. Front. Mol. Neurosci. 13, 21.
Huang, M., Wu, Y., Wang, N., Wang, Z., Zhao, P., Yang, X., 2014. Is the hypoglycemic action of vanadium compounds related to the suppression of feeding? Biol. Trace Elem. Res. 157, 242–248.
Huang, Y.Q., Wong, C.K., Zheng, J.S., Bouwman, H., Barra, R., Wahlström, B., et al., 2012. Bisphenol A (BPA) in China: a review of sources, environmental levels, and potential human health impacts. Environ. Int. 42, 91–99.
Hussain Shah, S.Z., Naveed, A.K., Rashid, A., 2016. Effects of oral vanadium on glycaemic and lipid profile in rats. J. Pak. Med. Assoc. 66 (12), 1592–1596.
Igado, O.O., Andrioli, A., Azeez, I.A., Girolamo, F., Errede, M., Aina, O.O., et al., 2020. The ameliorative effects of a phenolic derivative of Moringa oleifera leave against vanadium-induced neurotoxicity in mice. IBRO Rep. 9, 164–182.
Imtiaz, M., Rizwan, M.S., Xiong, S., Li, H., Ashraf, M., Shahzad, S.M., et al., 2015. Vanadium, recent advancements and research prospects: a review. Environ. Int 80, 79–88.
Inadera, H., 2015. Neurological effects of bisphenol A and its analogues. Int. J. Med. Sci. 12 (12), 926.
John, N., Rehman, H., Razak, S., David, M., Ullah, W., Afsar, T., et al., 2019. Comparative study of environmental pollutants bisphenol A and bisphenol S on sexual differentiation of anteroventral periventricular nucleus and spermatogenesis. Repro Biol. Endocrinol. 17, 1, 0.
Juan, C.A., Pérez de la Lastra, J.M., Plou, F.J., Pérez-Lebeña, E., 2021. The chemistry of reactive oxygen species (ROS) revisited: outlining their role in biological macromolecules (DNA, Lipids and Proteins) and induced pathologies. Int. J. Mol. Sci. 22 (9), 4642.
Kang, L., Tian, M.K., Bailey, C.D.C., Lambe, E.K., 2015. Dendritic spine density of prefrontal layer 6 pyramidal neurons in relation to apical dendrite sculpting by nicotinic acetylcholine receptors. Front. Cell. Neurosci. 9, 398. https://doi.org/10.3389/fncel.2015.00398.
Kany, S., Vollrath, J.T., Relja, B., 2019. Cytokines in inflammatory disease. Int. J. Mol. Sci. 20 (23), 6008.
Kasai, H., 2023. Unraveling the mysteries of dendritic spine dynamics: Five key principles shaping memory and cognition. Proc. Jpn. Acad. Ser. B Phys. Biol. Sci. 99 (8), 254–305. https://doi.org/10.2183/pjab.99.018.
Kawato, S., 2004. Endocrine disrupters as disrupters of brain function: a neurosteroid viewpoint. Environ. Sci. 11 (1), 1–14.
Khan, A., Ikram, M., Muhammad, T., Park, J., Kim, M.O., 2019. Caffeine modulates cadmium-induced oxidative stress, neuroinflammation, and cognitive impairments by regulating Nrf-2/HO-1 in vivo and in vitro. J. Clin. Med. 8 (5), 680.
Khan, J., Salhotra, S., Goswami, P., Akhter, J., Jahan, S., Gupta, S., et al., 2019. Bisphenol A triggers axonal injury and myelin degeneration with concomitant neurobehavioral toxicity in C57BL/6J male mice. Toxicology 428, 152299.
Khan, J., Waseem, M., Kamble, K., Parvez, S., Banerjee, B.D., Gupta, S., Raisuddin, S., 2026. Role of bisphenol A in the aberrant activation of ionotropic glutamate transporters in the cerebral cortex and altered behavioral responses in C57BL/6J mice. Front. Toxicol. 7, 1680589. https://doi.org/10.3389/ftox.2025.1680589.
Kim, J., Sharma, R.P., 2006. Cadmium-induced apoptosis in murine macrophages is antagonized by antioxidants and caspase inhibitors. J. Toxicol. Environ. Health (Part A) 69 (12), 1181–1201.
Kirkland, R.A., Franklin, J.L., 2003. Bax, reactive oxygen, and cytochrome c release in neuronal apoptosis. Antioxid. Redox Signal 5, 589–596.
Kraeuter, A.K., Guest, P.C., Sarnyai, Z., 2019. The open field test for measuring locomotor activity and anxiety-like behavior. Methods Mol. Biol. 1916, 99–103.
Kweon, J.H., Kim, S., Lee, S.B., 2017. The cellular basis of dendrite pathology in neurodegenerative diseases. BMB Rep. 50 (1), 5–11. https://doi.org/10.5483/bmbrep.2017.50.1.131.
Ladagu, A.D., Olopade, F.E., Chazot, P., Oyagbemi, A.A., Ohiomokhare, S., Folarin, O.R., et al., 2023. Attenuation of vanadium-induced neurotoxicity in rat hippocampal slices (in vitro) and mice (in vivo) by ZA-II-05, a novel NMDA-receptor antagonist. Int. J. Mol. Sci. 24 (23), 16710. https://doi.org/10.3390/ijms242316710.
Lawal, A.T., Sharafadeen, A.O., Akinola, O.B., 2023. Neuromorphological and biochemical effects of co-exposure to bisphenol A and cadmium in insulin-resistant rats. J. Neurobehav. Sci. 10 (3), 74–81.
León, I.E., Butenko, N., Di Virgilio, A.L., Muglia, C.I., Baran, E.J., Cavaco, I., et al., 2014. Vanadium and cancer treatment: antitumoral mechanisms of three oxidovanadium (IV) complexes on a human osteosarcoma cell line. J. Inorg. Biochem. 134, 106–117. https://doi.org/10.1016/j.jinorgbio.2013.10.009.
Li, J., Yu, G., Wang, L., Zhang, W., Ke, W., Li, Y., Liu, D., Xie, K., Xu, Y., Cha, C., Guo, G., Zhang, J., 2025. Enriched environment rescues bisphenol A induced anxiety-like behavior and cognitive impairment by modulating synaptic plasticity. Ecotoxicol. Environ. Saf. 289, 117427. https://doi.org/10.1016/j.ecoenv.2024.117427.
Li, J., Yuan, J., 2008. Caspases in apoptosis and beyond. Oncogene 27, 6194–6206. https://doi.org/10.1038/onc.2008.297.
Liu, M., Deng, P., Li, G., Liu, H., Zuo, J., Cui, W., et al., 2024. Neurotoxicity of combined exposure to the heavy metals (Pb and As) in zebrafish (Danio rerio). Toxics 12 (4), 282. https://doi.org/10.3390/toxics12040282.
Liu, W.Z., Zhang, W.H., Zheng, Z.H., Zou, J.X., Liu, X.X., Huang, S.H., et al., 2020. Identification of a prefrontal cortex-to-amygdala pathway for chronic stress-induced anxiety. Nat. Commun. 11, 2221. https://doi.org/10.1038/s41467-020-15920-7.
López, E., Arce, C., Oset-Gasque, M.J., Cañadas, S., González, M.P., 2006. Cadmium induces reactive oxygen species generation and lipid peroxidation in cortical neurons in culture. Free Radic. Biol. Med. 40, 940–951. https://doi.org/10.1016/j.freeradbiomed.2005.10.062.
Lowry, O.H., Rosebrough, N.J., Farr, A.L., Randall, R.J., 1951. Protein measurement with the Folin phenol reagent. J. Biol. Chem. 193 (1), 265–275.
Ma, Y., Liu, H., Wu, J., Yuan, L., Wang, Y., Du, X., et al., 2019. The adverse health effects of bisphenol A and related toxicity mechanisms. Environ. Res. 1 (176), 108575.
Mahdavi, S., Khodarahmi, P., Roodbari, N.H., 2018. Effects of cadmium on Bcl-2/ Bax expression ratio in rat cortex brain and hippocampus. Hum. Exp. Toxicol. 37 (3), 321–328. https://doi.org/10.1177/0960327117703687.
Manto, M., 2012. Toxic agents causing cerebellar ataxias. Handb. Clin. Neurol. 103, 201–213.
Manzoor, M.F., Tariq, T., Fatima, B., Sahar, A., Tariq, F., Munir, S., et al., 2022. An insight into bisphenol A, food exposure and its adverse effects on health: a review. Front. Nutr. 9, 1047827.
Meli, R., Monnolo, A., Annunziata, C., Pirozzi, C., Ferrante, M.C., 2020. Oxidative stress and BPA toxicity: an antioxidant approach for male and female reproductive dysfunction. Antioxidants (Basel) 9 (5), 405. https://doi.org/10.3390/antiox9050405.
Moens, U., Kostenko, S., Sveinbjørnsson, B., 2013. The role of mitogen-activated protein kinase-activated protein kinases (MAPKAPKs) in inflammation. Genes 4 (2), 101–133. https://doi.org/10.3390/genes4020101.
Moore, J.J., Rashid, S.K., Bicker, E., Johnson, C.D., Codrington, N., Chklovskii, D.B., Basu, J., 2025. Sub-cellular population imaging tools reveal stable apical dendrites in hippocampal area CA3. Nat. Commun. 16 (1), 1119. https://doi.org/10.1038/s41467-025-56289-9.
Moskalyk, R.R., Alfantazi, A.M., 2003. Processing of vanadium: a review. Min. Eng. 16, 793–805.
Mucci, F., Marazziti, D., Della Vecchia, A., Baroni, S., Morana, P., Carpita, B., et al., 2020. State-of-the-art: inflammatory and metabolic markers in mood disorders. Life 10, 82. https://doi.org/10.3390/life10060082.
Nabi, M., Tabassum, N., 2022. Role of environmental toxicants on neurodegenerative disorders. Front. Toxicol. 4, 837579.
Namura, S., Zhu, J., Fink, K., Endres, M., Srinivasan, A., Tomaselli, K.J., et al., 1998. Activation and cleavage of caspase-3 in apoptosis induced by experimental cerebral ischemia. J. Neurosci. 18, 3659–3668. https://doi.org/10.1523/JNEUROSCI.18-10-03659.1998.
Nayan, N.M., Husin, A., Sheikh Abd Kadir, S.H., Abd Aziz, C.B., Mazlan, M., Siran, R., 2022. Prenatal bisphenol A exposure impairs the aversive and spatial memory reduces the level of NMDA receptor subunits in the hippocampus of male Sprague Dawley rats. Brain Sci. Adv. 8 (1), 57–69. https://doi.org/10.26599/BSA.2022.9050009.
Oehlmann, J., Schulte-Oehlmann, U., Kloas, W., Jagnytsch, O., Lutz, I., Kusk, K.O., Wollenberger, L., Santos, E.M., Paull, G.C., Van Look, K.J.W., et al., 2009. A critical analysis of the biological impacts of plasticizers on wildlife. Philos. Trans. R. Soc. B-Biol. Sci. 364, 2047–2062. https://doi.org/10.1098/rstb.2008.0242.
Ojala, J.O., Sutinen, E.M., 2017. The role of interleukin-18, oxidative stress and metabolic syndrome in Alzheimer's disease. J. Clin. Med 6, 55. https://doi.org/10.3390/jcm6050055.
Olopade, J.O., Fatola, I.O., Olopade, F.E., 2011. Vertical administration of vanadium through lactation induces behavioural and neuromorphological changes: protective role of vitamin ENiger. J. Physiol. Sci. 26 (1), 55–60.

Pessoa, J.C., Etcheverry, S., Gambino, D., 2015. Vanadium compounds in medicine. Coord. Chem. Rev. 301–302, 24–48.
Petanjek, Z., Sedmak, D., Džaja, D., Hladnik, A., Rašin, M.R., Jovanov-Milosevic, N., 2019. The protracted maturation of associative layer IIIC pyramidal neurons in the human prefrontal cortex during childhood: a major role in cognitive development and selective alteration in autism. Front. Psych. 10, 122. https://doi.org/10.3389/fpsyt.2019.00122.
Putcha, G.V., Deshmukh, M., Johnson Jr, E.M., 1999. BAX translocation is a critical event in neuronal apoptosis: regulation by neuroprotectants, BCL-2, and caspases. J. Neurosci. 19, 7476–7485. https://doi.org/10.1523/JNEUROSCI.19-17-07476.1999.
Rao Barkur, R., Bairy, L.K., 2015. Evaluation of passive avoidance learning and spatial memory in rats exposed to low levels of lead during specific periods of early brain development. Int. J. Occup. Med Environ. Health 28 (3), 533–544. https://doi.org/10.13075/ijomeh.1896.00283.
Rauf, A., Khalil, A.A., Awadallah, S., Khan, S.A., Abu-Izneid, T., Kamran, M., et al., 2024. Reactive oxygen species in biological systems: pathways, associated diseases, and potential inhibitors—a review. Food Sci. Nut 12 (2), 675–693. https://doi.org/10.1002/fsn3.3784.
Rebuli, M.E., Camacho, L., Adonay, M.E., Reif, D.M., Aylor, D.L., Patisaul, H.B., 2015. Impact of low-dose oral exposure to bisphenol A (BPA) on juvenile and adult rat exploratory and anxiety behavior: a CLARITY-BPA consortium study. Toxicol. Sci. 148 (2), 341–354. https://doi.org/10.1093/toxsci/kfv163.
Rotruck, J.T., Pope, A.L., Ganther, H.E., Swanson, A.B., Hafeman, D.G., Hoekstra, W.G., 1973. Selenium: biochemical role as a component of glutathione peroxidase. Science (New York) 179 (4073), 588–590. https://doi.org/10.1126/science.179.4073.588.
Rozzo, C., Sanna, D., Garribba, E., Serra, M., Cantara, A., Palmieri, G., Pisano, M., 2017. Antitumoral effect of vanadium compounds in malignant melanoma cell lines. J. Inorg. Biochem 174, 14–24.
Sairanen, T., Szepesi, R., Karjalainen-Lindsberg, M.L., Saksi, J., Paetau, A., Lindsberg, P. J., 2009. Neuronal caspase-3 and PARP-1 correlate differentially with apoptosis and necrosis in ischemic human stroke. Acta Neuropathol. 118, 541–552. https://doi.org/10.1007/s00401-009-0559-3.
Sălcudean, A., Bodo, C.-R., Popovici, R.-A., Cozma, M.-M., Păcurar, M., Crăciun, R.-E., et al., 2025. Neuroinflammation—a crucial factor in the pathophysiology of depression—a comprehensive review. Biomolecules 15 (4), 502. https://doi.org/10.3390/biom15040502.
Sanchez, D.J., Colomina, M.T., Domingo, J.L., 1998. Effects of vanadium on activity and learning in rats. Physiol. Behav. 63 (3), 345–350.
Schünemann, K.D., Hattingh, R.M., Verhoog, M.B., Yang, D., Bak, A.V., Peter, S., van Loo, K.M.J., Wolking, S., Kronenberg-Versteeg, D., Weber, Y., Schwarz, N., Raimondo, J.V., Melvill, R., Tromp, S.A., Butler, J.T., Höllig, A., Delev, D., Wuttke, T. V., Kampa, B.M., Koch, H., 2025. Comprehensive analysis of human dendritic spine morphology and density. J. Neurophysiol. 133 (4), 1086–1102. https://doi.org/10.1152/jn.00622.2024.
Ścibior, A., Pietrzyk, Ł., Plewa, Z., Skiba, A., 2020. Vanadium: risks and possible benefits in the light of a comprehensive overview of its pharmacotoxicological mechanisms and multi-applications with a summary of further research trends. J. Trace Elem. Med. Biol. 61, 126508.
Sharma, R.P., Coulombe, R.A., Jr, Srisuchart, B., 1986. Effects of dietary vanadium exposure on levels of regional brain neurotransmitters and their metabolites. Biochem Pharm. 35 (3), 461–465. https://doi.org/10.1016/0006-2952(86)90220-0.
Shelby, M.D., 2008. NTP-CERHR monograph on the potential human reproductive and developmental effects of bisphenol A. Ntp Cerhr Mon. 22 v,vii–ix,1–64assim.
Soazo, M., Garcia, G., 2007. Vanadium exposure through lactation produces behavioral alterations and CNS myelin deficit in neonatal rats. Neurotoxicology and Teratology 29 (4), 503–510. https://doi.org/10.1016/j.ntt.2007.03.001.
Sun, L., Wang, K., Li, Y., Fan, Q., Zheng, W., Li, H., 2017. Vanadium exposure-induced striatal learning and memory alterations in rats. Neurotoxicol 62, 124–129.
Susiarjo, M., Xin, F., Stefaniak, M., Mesaros, C., Simmons, R.A., Bartolomei, M.S., 2017. Bile acids and tryptophan metabolism are novel pathways involved in metabolic abnormalities in BPA-exposed pregnant mice and male offspring. Endocrinol 158 (8), 2533–2542. https://doi.org/10.1210/en.2017-00046.
Tchounwou, P.B., Yedjou, C.G., Patlolla, A.K., Sutton, D.J., 2012. Heavy metal toxicity and the environment. Exp. Suppl. 101, 133–164. https://doi.org/10.1007/978-3-7643-8340-4_6.
Tran, N.Q.V., Miyake, K., 2017. Neurodevelopmental disorders and environmental toxicants: epigenetics as an underlying mechanism. Int. J. Genom., 7526592 https://doi.org/10.1155/2017/7526592.
Umukoro, S., Ajayi, A.M., Ben-Azu, B., Ademola, A.P., Areelu, J., Orji, C., Okubena, O., 2023. Jobelyn® improves motor dysfunctions induced by haloperidol in mice via neuroprotective mechanisms relating to modulation of cAMP response-element binding protein and mitogen-activated protein kinase. Metab. Brain Dis. 38 (7), 2269–2280. https://doi.org/10.1007/s11011-023-01253-z.
Wang, C., He, C., Xu, S., Gao, Y., Wang, K., Liang, M., Hu, K., 2024. Bisphenol A triggers apoptosis in mouse pre-antral follicle granulosa cells via oxidative stress. J. Ovarian Res. 17 (1), 20. https://doi.org/10.1186/s13048-023-01322-y.
Wang, P., Nolan, T.M., Yin, Y., Bassham, D.C., 2020. Identification of transcription factors that regulate ATG8 expression and autophagy in Arabidopsis. Autophagy 16, 123–139.
Wang, S., Shi, X., 2001. Molecular mechanisms of metal toxicity and carcinogenesis. Mol. Cell Biochem 222, 3–9.
Yang, M., Fan, Z., Xie, Y., Fang, L., Wang, X., Yuan, Y., Li, R., 2020. Transcriptome analysis of the effect of bisphenol A exposure on the growth, photosynthetic activity and risk of microcystin-LR release by Microcystis aeruginosa. J. Hazard Mater. 397, 122746.
Zhang, J., Li, X., Zhou, L., Wang, L., Zhou, Q., Huang, X., 2016. Analysis of effects of a new environmental pollutant, bisphenol A, on antioxidant systems in soybean roots at different growth stages. Sci. Rep. 6, 23782.
Zhenkun, L., Wang, L., Jia, Y., Yanfang, Z., Qiaoxiang, D., Hung, C., 2017. A study on environmental bisphenol A pollution in plastics industry areas. Water Air Soil Pollut. 228, 1–9.
Zhu, X., Cao, L., Liu, Y., Tang, X., Miao, Y., Zhang, J., et al., 2024. Genotoxicity of bisphenol AF in rats: detrimental to male reproductive system and probable stronger micronucleus induction potency than BPA. J. Appl. Toxicol. 44 (3), 428–444. https://doi.org/10.1002/jat.4552.
Zwolak, I., 2020. The role of selenium in arsenic and cadmium toxicity: an updated review of scientific literature. Biol. Trace Elem. Res 193 (1), 44–63. https://doi.org/10.1007/s12011-019-01691-w.